Check for updates

Journal of Applied Mathematics

WILEY

RESEARCH ARTICLE OPEN ACCESS

Analysis of a Mathematical Model on the Dynamics of TB–HCV Coinfection With Medication

Kizito Mohammed[1] | Hasifa Nampala[2] | Pius Ariho[1]

[1]Department of Mathematics, Mbarara University of Science and Technology, P.O. Box 1410, Mbarara, Uganda | [2]Department of Mathematics and Statistics, Kyambogo University, P.O. Box 1, Kyambogo, Uganda

Correspondence: Kizito Mohammed (kmohammed@must.ac.ug)

Received: 10 June 2024 | **Revised:** 18 January 2026 | **Accepted:** 20 January 2026

Academic Editor: Theodore Simos

Keywords: coinfection | deterministic model | effective reproduction number | hepatitis C | tuberculosis

ABSTRACT

This study employs a deterministic model that describes the combined dynamics of TB and HCV aimed at determining the impact of medication in the management of TB–HCV coinfection. The analytical and numerical analyses indicate that if the TB–HCV coinfection effective reproduction number is less than unity, the absence of both TB and HCV infections constitutes a stable equilibrium. Additionally, the stability analysis reveals that when the TB–HCV coinfection effective reproduction number is greater than one, the endemic equilibria become stable attractors, thus, a long-term coexistence of both infections. Sensitivity analysis shows that an increase in the rate of human-to-human contact between the TB (or HCV)-infected individuals and the susceptible population and the likelihood of a contact resulting in TB (or HCV) transmission results in a higher endemicity of the infection. Numerical simulations indicate that increasing the rate at which humans with coinfection are treated decreases the widespread presence of TB and HCV in the population. We therefore recommend that health facilities be stocked with antibiotics for TB and antiviral medications for HCV for easy access by individuals who test positive to the respective infections.

1 | Introduction

Tuberculosis (TB) is a transmissible disease resulting from *Mycobacterium tuberculosis* (Mtb) infection. The disease is estimated to cause death of about one million people globally each year [1]. TB affects the respiratory system (pulmonary TB) and also affects other body parts (extrapulmonary TB), except the hair and the nails.

The mode of transmission of TB is through breathing in droplets from cough or sneeze from infected person especially with infectious TB. Infectious TB persons show the visible clinical symptoms such as loss of weight, chronic cough, sputum production and night sweat among others. However, the TB-infected persons without these symptoms are called latent TB-infected persons. The latent TB-infected persons are noninfectious [2]. The latent period measures the time from infection to the point at which the individual becomes infectious to others and can persist for varying duration, ranging from weeks to months to a lifetime [2, 3].

Infectious TB in individuals can be detected by blood test or skin test, followed by treatment.

Drugs for effective medical treatment for TB have been used since the early 40s when they were first developed. The treatment regimen recommended by WHO has kept on being revised from time to time in light of more developments in the field of medicine and cognisant of the fact that the microorganisms keep evolving to some strains of microorganisms that show resistance.

The 2022 WHO guidelines [4] recommend a 4-drug regimen of isoniazid (H), rifampicin (R), ethambutol (E) and pyrazinamide (Z) for six months, as the latest treatment strategy for individuals

This is an open access article under the terms of the Creative Commons Attribution License, which permits use, distribution and reproduction in any medium, provided the original work is properly cited.

Copyright © 2026 Kizito Mohammed et al. *Journal of Applied Mathematics* published by John Wiley & Sons Ltd.

with drug-susceptible TB (both pulmonary and extrapulmonary). New further recommendations include, for children 12 years and above with pulmonary TB, that is, susceptible to drugs may receive treatment with regimen rifapentine (P), H, Z, and moxifloxacin (M) for 4 months; children and adolescents in the 3 months to 16 years age group with nonsevere TB may receive a 4-month treatment with regimen (2 months of H, R, Z and also E then followed by 2 months of H and R) as long as there is no evidence of resistance to R and H.

The majority of WHO member states typically reports treatment success rates of at least 85% for individuals on the 6-month regimen [4].

Hepatitis C virus (HCV) is the most severe strain of hepatitis virus that affects the liver (by inflaming it). HCV is classified under the genus Hepacivirus and family Flaviviridae. In addition to HCV, Flaviviridae family comprises other significant viruses like West Nile, yellow fever and dengue [5]. HCV is a blood-borne pathogen transmitted via blood transfusion or contact with infected blood from an infected person to a noninfected person. Blood contact can happen mostly through sharing needles, congenital transmission (mother to child during labour or nursing), organ transplants with unscreened organs and through unprotected sexual contacts [6].

HCV causes both acute (short term) and chronic hepatitis (long term illness). Some people with acute hepatitis C do not show symptoms or show mild symptoms of the disease within 6 months of exposure and may not need hospitalisation [7]. Untreated chronic HCV can result in long term and potentially health consequences such as liver cirrhosis, cancer and death [8].

As stated in 2019 report by WHO, close to 58 million people globally had chronic HCV infection and were continuing to live with it. Approximately 400,000 deaths occur every year due to chronic diseases caused by HCV infection. As a result, HCV infection is considered a significant public health concern. There is a likelihood of advancing to various stages of the disease on getting infected with HCV. A comprehensive guide for the prevention, treatment and epidemiological management of HCV infection specifically targeting people who inject drugs (PWID) indicates that out of every 100 people living with HCV infection, up to 80%, 70% and 20% will potentially progress to chronic HCV infection, chronic liver disease and cirrhosis, respectively, and up to 5% are at a risk of fatal cirrhosis or liver cancer [9]. The global health sector sets a goal to eliminate viral hepatitis with a substantial decreased public threat, with a 90% decrease in global cases and 65% decline in death [10].

Unlike TB infections, which manifest easily and necessitate seeking medication, infections with HCV take longer to manifest. Thus, humans with HCV are usually not informed that they are sick of HCV until a few years later [11, 12], hence, hardly quest medication. It is worth noting therefore that globally, medical check-up, clinical diagnosis and medication of hepatitis C sick persons are still a challenge.

A report on global hepatitis of 2021 [13] revealed that between 2015–2019, of the about 58 million people living with HCV, only 26% had undergone diagnostic tests for hepatitis C and were aware of their status (Africa had the least ratio of 6% diagnosed), 7% commenced medication and 7.7% cumulatively had ever been treated of HCV through the use of direct-acting antiviral (DAAs) medications.

In developed countries, it is mandatory for every TB sick person to be checked for HCV on admission into the health system which is not the case with most resource limited countries in sub-Saharan Africa. This is attributed to high cost of HCV screening and medication. According to [14, 15], medical check-up of HCV becomes important while establishing whether HCV could possibly lead to liver disease with TB sick persons.

TB and hepatitis C and their coinfection are among the most serious public health issues globally. Analysing the interconnected dynamics of TB and HCV infections is mathematically a significant challenge as the transmission routes for the infections are vastly different. Individuals with existing TB infection are at a greater likelihood of developing chronic HCV infection, which in turn increases their risk of experiencing liver damage (hepatotoxicity) as a side effect of certain medications [16, 17]. TB and HCV coinfection can trigger latent TB reactivation, heightens the risk of fatal outcomes and causes liver damage due to the drug toxicity [18]. Generally, HCV-coinfected individuals with TB are complicated to manage, which increases the possibility of passing on TB to others.

Also, the majority of the TB-infected individuals are HIV infected too. Therefore, indirectly, it is possible that one is dealing with TB–HCV–HIV trio infection, indicating a high load of medication. These individuals thus need a health liver to deal with all the medication of the trio infection of TB, HCV and HIV. Various mathematical modelling approaches have been employed to comprehend the dynamics of infectious diseases such as TB cynics [3, 19–22], HCV infection [9, 11, 12, 23], hepatitis B virus infection [24] and coinfection scenarios as discussed below: Nino et al. [25] conducted a study to determine whether HCV coinfection increases the risk of incident drug-induced hepatitis among patients on first-line anti-TB drug therapy. A high prevalence of HCV coinfection was found among patients with TB infection. Drug-induced hepatotoxicity is significantly associated with HCV coinfection but severe drug-induced hepatotoxicity is rare. El-Mokhtar et al. [26] conducted a study to evaluate the impact of HCV on the T-cell-mediated immune response to TB in coinfected patients. They concluded that different subsets of TB-specific $CD4^+$ T cells in TB–HCV-infected individuals are partially impaired in early-stage HCV infection. Meysam et al. [18] carried out a systematic review and meta-analysis with a purpose of determining the prevalence of HCV infection in patients with TB infection. The results of their study highlighted the importance of screening HCV in TB patients. Knowing whether HCV is present or not in these patients can be helpful in effectively treating them. Musso et al. [27] conducted a study to assess the feasibility and effectiveness of simultaneous treatment for HCV infection and pulmonary multidrug-resistant TB (MDR-TB). In their study, they described two cases of patients with pulmonary MDR-TB and concurrent HCV chronic infection cured with DAAs at a Tertiary Infectious Diseases Hospital in Italy. They concluded by suggesting to always considering treatment of chronic hepatitis C with DAAs as a useful intervention for reintroduction of second-line antitubercular agents in those patients who developed drug-induced liver injury, reducing the risk of treatment interruption when re-exposed to these drugs. To assess the prevalence of HCV infection among TB

4185, 2026, 1, Downloaded from https://onlinelibrary.wiley.com/doi/10.1155/jama/8033235 by Readcube (Labtiva Inc.), Wiley Online Library on [12/11/2026]. See the Terms and Conditions (https://onlinelibrary.wiley.com/terms-and-conditions) on Wiley Online Library for rules of use; OA articles are governed by the applicable Creative Commons License

patients and to investigate its impact on TB and its treatment outcome, Nageeb et al. [28] carried out a cross-sectional study on 500 TB patients. They revealed that coinfection of HCV in patients with TB is frequent. It increases the frequency of almost all clinical presentations and had its predominant findings on laboratory and radiological investigations. Coinfection also alters the response to TB treatment and should be screened among tuberculous patients before treatment and closely monitored during treatment to detect early any drug resistance or treatment failure. Wahid et al. [29] carried out a study aimed at suggesting proper management of patients coinfected with both HCV and TB infections. According to their results, this is the first evidence that highlights sofosbuvir, daclatasvir and ribavirin as an optimal treatment regimen for patients coinfected with TB infection. Furthermore, it is necessary to treat TB infection before initiating HCV treatment because of the risk of hepatotoxicity. Kempker et al. [30] reviewed the drug metabolism of anti-TB and HCV drugs and the known potential drug–drug interactions between recommended HCV regimens and individual anti-TB drugs. They realised that rifampin is the only anti-TB drug to have been formally studied for potential drug interactions with anti-HCV DAAs, and existing data preclude these combinations. They, however, discovered that based on known pathways of drug metabolism and enzyme effects, the combination of HCV DAA regimens with all other anti-TB drugs may be feasible. In their conclusion, pharmacokinetic studies are needed next to help move cotreatment regimens forward for clinical use among patients coinfected with TB and HCV infections. Aggarwal [31] developed a nonlinear mathematical model for HIV–TB coinfection. They introduced a time-delay parameter to capture the delay in diagnosis and treatment initiation for coinfected individuals. The local stability analysis of equilibrium points was analysed in the presence of delay, revealing specific conditions for Hopf bifurcation to occur. Numerical simulations were carried out using different parameter sets to examine the effects of detection and treatment delays on coinfected individuals at each equilibrium point. Bowong et al. [32] formulated and analysed a deterministic mathematical model of the codynamics of HBV/TB coinfection. Through simulations, they mainly found that the two diseases will coexist whenever their partial reproductive numbers exceed unity; the increased progression rate due to exogenous reinfection from latent to active TB in coinfected individuals may play a significant role in the rising prevalence of TB and the increased progression rates from acute stage to chronic stage of HBV infection and has increased the prevalence levels of HBV and TB. Tanvi et al. [33] formulated and analysed an HIV–TB coinfection model which incorporated a nonlinear treatment rate for TB infection. They developed an HIV–TB coinfection model, analysing the HIV and TB submodels separately, and calculated the basic reproduction numbers for HIV-only, TB-only, and the full HIV–TB coinfection model. Numerical simulations showed that accelerating TB treatment can effectively reduce the coinfection, highlighting the need for programs that enhance TB treatment rates. Bhunu et al. [34] formulated and analysed a deterministic model of the codynamics of HCV and HIV/AIDS in order to assess their impact on the dynamics of each disease in the presence of treatment. They realised that there are more HIV-only infected individuals not yet showing AIDS symptoms and the number of dually infected individuals first increases and then declines to asymptotically low level due to full recovery from hepatitis C. In their conclusion, HCV has an ongoing prolonged negative effect on the health of the population, irrespective of their HIV status, and as such, its control should be reinforced in resource-limited settings. Teklu et al. [35] developed and analysed a compartmental model with optimal control strategies to examine the dynamics of HIV/AIDS-TB coinfection, incorporating behavioural changes and treatment interventions. The numerical simulations demonstrate that a strategically combined approach of preventive and therapeutic interventions can effectively curtail the incidence of HIV, TB and coinfection with HIV/AIDS-TB. Mayanja et al. [16] formulated and analysed a deterministic model to study the HIV–HCV coinfection dynamics in the presence of HIV therapy. The results indicated that both HIV and HCV infections enhance each other; and in the long run, increasing the rates at which people are put on HIV treatment reduces the prevalence of HCV in the community; however, it increases the prevalence of HIV. Nampala et al. [36], proposed a coinfection mathematical model with delay and used optimal control theory to analyse the effect of viral latency in hepatocytes on the dynamics of HIV/HBV coinfection. Analytical results indicate that HBV cannot take a competitive exclusion against HIV; thus, the coinfection endemic equilibrium implies chronic HBV in HIV-infected patients. Teklu et al. [37] formulated and analysed a dynamical system modelling HBV and TB coinfection to investigate the impact of optimal control measures and conducted a cost-effectiveness analysis, aiming to inform strategies to control coinfection transmission. Their findings indicate that a combined approach of protective and treatment optimal control strategies effectively reduces the incidence of HBV and TB coinfection. Furthermore, cost-effectiveness analysis reveals that treating HBV is the most cost-effective strategy to combat the spread of HBV and TB coinfection in the community. Tanvi et al. [38] formulated a nonlinear population model for HIV–TB coinfection. Their model examined how the timing of HIV treatment initiation (early or late) in TB-treated coinfected individuals influenced the incidence of immune reconstitution inflammatory syndrome (IRIS). With fixed control parameters, the model analysis demonstrated the existence and local stability of disease-free and endemic equilibria. They formulated and solved an optimal control problem incorporating time-dependent parameters, using Pontryagin's maximum principle to minimise the number of infected individuals, disease-induced deaths and treatment costs. Numerical results suggested that implementing optimal control strategies is more effective than constant treatment rates in minimising the burden of the coinfection. In a recent study, Kizito et al. [39] formulated and analysed a deterministic model to examine the dynamics of TB and HCV coinfection without interventions, shedding light on the underlying mechanisms driving the coinfection's behaviour. The results showed that, over time, the number of individuals coinfected with TB and HCV significantly exceeded the number in any other demographic group. In the absence of interventions, the dynamics of TB and HCV coinfection were primarily driven by TB. This study advances the previous research in [39] by incorporating TB and HCV treatment and examining the dynamics of TB–HCV coinfection under the influence of both treatments. The model in this study provides new insights through a novel mathematical modelling approach that highlights the crucial role of treatment in reducing the transmission of TB and HCV infections, addressing a previously unexplored research area, thus ultimately providing policymakers with

4185, 2026, 1, Downloaded from https://onlinelibrary.wiley.com/doi/10.1155/jama/8033235 by Readcube (Labtiva Inc.), Wiley Online Library on [12/11/2026]. See the Terms and Conditions (https://onlinelibrary.wiley.com/terms-and-conditions) on Wiley Online Library for rules of use; OA articles are governed by the applicable Creative Commons License

evidence-based interventions to reduce the spread of both infections..

2 | Description and Formulation of the Model

2.1 | Description of the TB–HCV Coinfection Dynamics

The model categorises the human population into 13 distinct and separate groups ascending to their epidemiological status, namely susceptible individuals capable of acquiring TB or HCV ($S(t)$), TB infected, latent and not contagious ($I_L(t)$), TB infectious individuals ($I_T(t)$), TB infectious hospitalised individuals on medication ($H(t)$), TB-treated individuals ($R_T(t)$), HCV acutely infectious individuals but with no symptoms ($I_A(t)$), HCV chronically infectious individuals with symptoms ($I_C(t)$), HCV individuals under treatment ($R_H(t)$), individuals with acute HCV infection and latent TB, not infectious with TB but infectious with HCV ($I_{AL}(t)$), dually infected humans with HCV chronic infection in the latent TB stage, noninfectious for TB but infectious for HCV ($I_{CL}(t)$), individuals with acute HCV infection in the infectious stage of TB ($I_{AT}(t)$), individuals with chronic HCV infection in infectious stage of TB ($I_{CT}(t)$) and individuals under treatment of the dual infection ($R(t)$).

The medication for HCV patients shall be considered only at the HCV chronic stage. This is because HCV acute stage is often short and asymptomatic in relation to the lengthy and symptomatic HCV chronic stage. Thus, diagnosis of HCV patients is at the chronic phase of the infection [40].

In order to formulate the dynamical system, all susceptible individuals are assumed to be just as susceptible to both TB and HCV, and the diseases are spread by contact with an infected individual. TB-infected individuals first get latently infected and go on to become infectious. However, TB latent individuals are not infectious. Similarly, before developing chronic HCV, all hepatitis C virus–infected persons first contract acute HCV, and both forms of HCV are infectious. Acute HCV individuals either advance to the chronic stage or recover naturally. However, since the acute form of HCV is primarily asymptomatic, there is hardly any possibility of medication at this stage. TB- and hepatitis C-recovered humans acquire temporary immunity before reinfection.

The total population at time t, represented by $N(t)$, is defined as

$$N(t) = S(t) + I_L(t) + I_T(t) + H(t) + R_T(t) + I_A(t) + I_C(t) + R_H(t) + I_{AL}(t) + I_{CL}(t) + I_{AT}(t) + I_{CT}(t) + R(t). \quad (1)$$

No matter when, there is a steady inflow into the susceptible class, $S(t)$, through birth and immigration at a rate Λ. A constant natural mortality rate, μ, exists in all subpopulations.

Susceptible humans acquire TB to move to latent TB class, $I_L(t)$, at a rate λ_T defined by

$$\lambda_T(t) = \frac{\xi_1 q_1 (I_T(t) + \epsilon H(t) + a(I_{AT}(t) + I_{CT}(t)))}{N(t)}, \quad (2)$$

with ξ_1 the rate of human-to-human contact between the TB-infected individuals and susceptible population; q_1 is the likelihood of a contact resulting in TB transmission; a is the enhancement factor for the increased risk of easily contracting TB from a dually infected human in classes I_{AT} and I_{CT}. The parameter accounts for increased infectiousness in dually infected humans compared to those with TB only [32].

ϵ is the reduction parameter considering for the reduced risk of being infected with TB by a hospitalised TB-infected human.

Similarly, susceptible humans get infected with HCV to move to the acute class, $I_A(t)$, at a rate λ_H, defined by (3).

$$\lambda_H(t) = \frac{\xi_2 q_2 (\phi I_A(t) + I_C(t) + b_1 I_{AL}(t) + b_2 I_{CL}(t) + b_3 I_{AT}(t) + b_4 I_{CT}(t))}{N(t)}, \quad (3)$$

where ξ_2 is the rate of human-to-human contact between the HCV-infected individuals and susceptible population; q_2 is the likelihood of a contact resulting in HCV transmission; b_1, b_2, b_3 and b_4 are enhancement factors for the increased risk of easily contracting HCV from a dually infected individual in classes I_{AL}, I_{CL}, I_{AT} and I_{CT}, respectively. Dual-infected individuals are more infectious of HCV as compared to their counterparts who are monoinfected. We note that $b_1, b_3 > b_2, b_4 > 1$, considering the fact that an HCV acutely infected human is more infectious than the HCV chronically infected human due to higher viral loads during the early stages of the infection. ϕ is the amplification parameter catering for the increased risk of being infected with HCV from a singly acute HCV-infected individual.

TB latently infected humans, I_L, either recover naturally due to strong immune system at a rate η to return to susceptible class or progress to active TB class, $I_T(t)$, at a rate θ.

Once humans infected with active TB are tested positive, some are put on medication while attended to from home at a rate ω_1 to join the $R_T(t)$ class, whereas others are hospitalised at a rate ρ to join the $H(t)$ class while, in hospital, the active TB patients receive treatment at a rate ω_2 to also join the $R_T(t)$ class.

Individuals in classes $I_T(t)$ and $H(t)$ not only die naturally but also die from active TB at a rate σ_1 and σ_2, respectively.

Acute HCV humans that happen to recover naturally return to the susceptible class at a rate π, while others progress to the chronic HCV class, $I_C(t)$, at a rate α. Having been detected with chronic HCV, the infected humans are put on treatment at a rate ψ to join the $R_H(t)$ class.

Latent TB and active TB individuals in classes $I_L(t)$ and $I_T(t)$, respectively, at a rate of λ_H, become infected with HCV and transit to state $I_{AL}(t)$ and $I_{AT}(t)$, respectively. Similarly, acute and chronic HCV humans in classes $I_A(t)$ and $I_C(t)$ are infected with TB at a rate λ_T to join classes $I_{AL}(t)$ and $I_{CL}(t)$, respectively.

Humans in I_{AL} progress to $I_{AT}(t)$ and $I_{CL}(t)$ at rates τ_1 and β_1, respectively. Similarly, humans in classes $I_{CT}(t)$ and $I_{AL}(t)$ both progress to $I_{CT}(t)$ class at rates τ_2 and β_2, respectively. Having tested positive to the coinfection, humans in classes $I_{CL}(t)$, $I_{AT}(t)$ and $I_{CT}(t)$ are put on treatment at rates r_1, r_2 and r_3 to join $R(t)$ class.

In addition to natural death, humans in $I_C(t)$ and $I_{CL}(t)$ classes also die from chronic HCV-induced death at a rate δ, and those in

4185, 2026, 1, Downloaded from https://onlinelibrary.wiley.com/doi/10.1155/jama/8033235 by Readcube (Labtiva Inc.), Wiley Online Library on [12/11/2026]. See the Terms and Conditions (https://onlinelibrary.wiley.com/terms-and-conditions) on Wiley Online Library for rules of use; OA articles are governed by the applicable Creative Commons License

classes $I_{AT}(t)$ and $I_{CT}(t)$ also die from coinfection-induced death at rates d_1 and d_2, respectively.

Because previous infection does not provide permanent immunity, humans in classes $R_H(t)$, $R_T(t)$ and $R(t)$ return to susceptible class having been treated to clearance of the infection at rates ν_1, ν_2 and ν_3, respectively.

The TB–HCV coinfection model is depicted in Figure 1 as a compartmental diagram.

2.1.1 | Equations of the Model

Using the compartmental model shown in Figure 1 and the parameters provided in Table 1, the model is derived on the basis of the descriptions above using first-order nonlinear ordinary differential equations as follows:

$$\begin{aligned}
\frac{dS(t)}{dt} &= \Lambda + \nu_1 R_H(t) + \nu_2 R_T(t) + \nu_3 R(t) + \pi I_A(t) \\
&\quad + \eta I_L(t) + \gamma I_{AL}(t) - (\lambda_T + \lambda_H + \mu)S(t), \\
\frac{dI_L(t)}{dt} &= \lambda_T S(t) + p_1 \pi I_{AL}(t) - (\theta + \eta + \mu + \lambda_H)I_L(t), \\
\frac{dI_T(t)}{dt} &= \theta I_L(t) - (\omega_1 + \rho + \mu + \sigma_1 + \lambda_H)I_T(t), \\
\frac{dH(t)}{dt} &= \rho I_T(t) - (\omega_2 + \mu + \sigma_2)H(t), \\
\frac{dR_T(t)}{dt} &= \omega_2 H(t) + \omega_1 I_T(t) - (\nu_2 + \mu)R_T(t), \\
\frac{dI_A(t)}{dt} &= \lambda_H S(t) + p_2 \eta I_{AL}(t) - (\pi + \alpha + \mu + \lambda_T)I_A(t), \\
\frac{dI_C(t)}{dt} &= \alpha I_A(t) - (\psi + \mu + \delta + \lambda_T)I_C(t), \\
\frac{dR_H(t)}{dt} &= \psi I_C(t) - (\nu_1 + \mu)R_H(t), \\
\frac{dI_{AL}(t)}{dt} &= \lambda_T I_A(t) + \lambda_H I_L(t) \\
&\quad - (\tau_1 + \mu + \beta_1 + \gamma + p_1\pi + p_2\eta)I_{AL}(t), \\
\frac{dI_{CL}(t)}{dt} &= \beta_1 I_{AL}(t) + \lambda_T I_C(t) - (r_1 + \tau_2 + \mu + \delta)I_{CL}(t), \\
\frac{dI_{AT}(t)}{dt} &= \tau_1 I_{AL}(t) + \lambda_H I_T(t) - (r_2 + \beta_2 + \mu + d_1)I_{AT}(t), \\
\frac{dI_{CT}(t)}{dt} &= \tau_2 I_{CL}(t) + \beta_2 I_{AT}(t) - (r_3 + \mu + d_2)I_{CT}(t), \\
\frac{dR(t)}{dt} &= r_1 I_{CL}(t) + r_2 I_{AT}(t) + r_3 I_{CT}(t) - (\nu_3 + \mu)R(t),
\end{aligned} \tag{4}$$

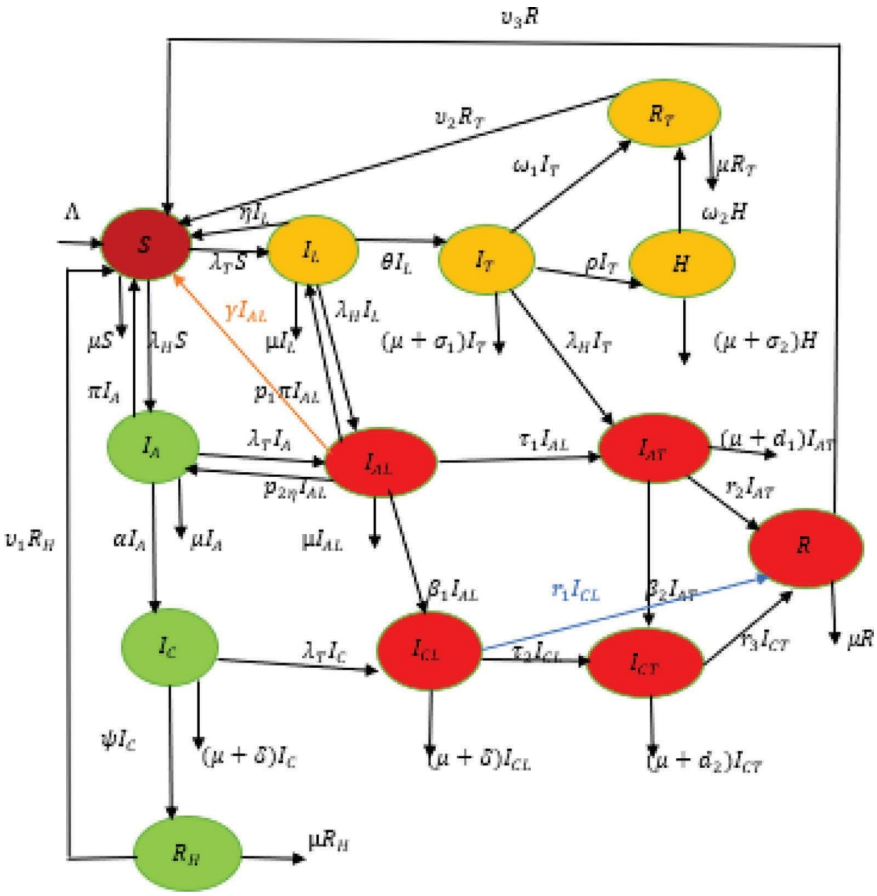


FIGURE 1 | The compartmental model diagram for TB–HCV coinfection.

4185, 2026, 1, Downloaded from https://onlinelibrary.wiley.com/doi/10.1155/jama/8033235 by Readcube (Labtiva Inc.), Wiley Online Library on [12/11/2026]. See the Terms and Conditions (https://onlinelibrary.wiley.com/terms-and-conditions) on Wiley Online Library for rules of use; OA articles are governed by the applicable Creative Commons License

TABLE 1 | Parameters used in the model formulation and their description.

Parameter	Definition
Λ	Per capita recruitment rate into susceptible population
μ	Natural mortality rate
σ_1	Mortality rate for individuals with infectious TB
σ_2	Mortality rate for individuals hospitalised with infectious TB
δ	Mortality rate for individuals with chronic form of HCV
d_1	Mortality rate due to infectious TB in individuals with acute HCV and infectious TB
d_2	Mortality rate due to either chronic HCV or infectious TB
θ	Rate of progression from latent to infectious TB
ρ	Rate at which the TB infectious individuals are hospitalised
ω_1	Rate at which TB infectious individuals are put on treatment
ω_2	Rate at which hospitalised infectious TB individuals are put on treatment
α	Progression rate from acute class to chronic HCV class
τ_1	Progression rate from I_{AL} class to I_{AT} class
τ_2	Progression rate from I_{CL} class to I_{CT} class
β_1	Progression rate from I_{AL} class to I_{CL} class
β_2	Progression rate from I_{AT} class to I_{CT} class
ψ	Rate at which chronic HCV individuals are put on treatment
r_1	Rate at which individuals in I_{CL} class are put on HCV treatment
r_2	Rate at which individuals in I_{AT} class are put on TB treatment
r_3	Rate at which individuals in I_{CT} class are put on treatment
ν_1	Rate of loss of temporary immunity to HCV
ν_2	Rate of loss of temporary immunity to TB
ν_3	Rate of loss of temporary immunity to both TB and HCV
η	Rate of natural recovery of latent TB individuals
π	Rate of natural recovery of acute HCV individuals
ϵ	Transmission coefficient for the hospitalised individuals
ϕ	Transmission coefficient for the HCV acute individuals
γ	Natural clearance of both acute HCV and latent TB in I_{AL} class
p_1	Reduction parameter for reduced natural acute HCV clearance in I_{AL} class
p_2	Reduction parameter for reduced natural latent TB clearance in I_{AL} class

where λ_T and λ_H are as described in (2) and (3), respectively. The variables of the system are initially set at

$$\begin{aligned} &S(0) > 0, I_L(0) \geq 0, I_T(0) \geq 0, H(0) \geq 0, R_T(0) \geq 0, \\ &I_A(0) \geq 0, I_C(0) \geq 0, R_H(0) \geq 0, I_{AL}(0) \geq 0, \\ &I_{CL}(0) \geq 0, I_{AT}(0) \geq 0, I_{CT}(0) \geq 0, \text{ and } R(0) \geq 0. \end{aligned} \tag{5}$$

3 | Analysis of the Model

3.1 | Positivity and Boundedness of TB–HCV Coinfection Model Solutions

Since the model system (4) studies human population, we need to verify that the model system is both mathematically well-defined and biologically relevant.

In this subsection, we analyse the solution properties of the TB–HCV coinfection model (4) focussing on positivity and boundedness.

Theorem 1 (positivity of solutions). *The solutions* $S(t)$, $I_L(t)$, $I_T(t)$, $H(t)$, $R_T(t)$, $I_A(t)$, $I_C(t)$, $R_H(t)$, $I_{AL}(t)$, $I_{CL}(t)$, $I_{AT}(t)$, $I_{CT}(t)$ *and* $R(t)$ *of the model System (4) are positive for* $t \geq 0$.

Proof 1. Let the starting values of the variables of System (4) be as defined in Equation (5). Each component of the system's solution is demonstrated to be non-negative. Assuming the contrary, we suppose that there exists a first instant t_1: $S(t_1) = 0, S'(t_1) < 0 \text{ and } S(t) > 0, I_L(t) > 0, \ldots, R(t) > 0 \text{ for } 0 < t < t_1$ or there exists a t_2: $I_L(t_2) = 0, I_L'(t_2) < 0 \text{ and } S(t) > 0, I_L(t) > 0, \ldots, R(t) > 0 \text{ for } 0 < t < t_2$ or there exists a t_3: $I_T(t_3) = 0, I_T'(t_3) < 0 \text{ and } S(t) > 0, I_L(t) > 0, \ldots, R(t) > 0 \text{ for } 0 < t < t_3$ or there exists a t_4: $H(t_4) = 0, H'(t_4) < 0 \text{ and } S(t) > 0, I_L(t) > 0, \ldots, R(t) > 0 \text{ for } 0 < t < t_4$ or there exists a t_5: $R_T(t_5) = 0, R_T'(t_5) < 0 \text{ and } S(t) > 0, I_L(t) > 0, \ldots, R(t) > 0 \text{ for } 0 < t < t_5$ or there exists a t_6: $I_A(t_6) = 0, I_A'(t_6) < 0$ and $S(t) > 0, I_L(t) > 0, \ldots, R(t) > 0 \text{ for } 0 < t < t_6$ or there exists a t_7: $I_C(t_7) = 0, I_C'(t_7) < 0 \text{ and } S(t) > 0, I_L(t) > 0, \ldots, R(t) > 0 \text{ for } 0 < t < t_7$ or there exists

4185, 2026, 1, Downloaded from https://onlinelibrary.wiley.com/doi/10.1155/jama/8033235 by Readcube (Labtiva Inc.), Wiley Online Library on [12/11/2026]. See the Terms and Conditions (https://onlinelibrary.wiley.com/terms-and-conditions) on Wiley Online Library for rules of use; OA articles are governed by the applicable Creative Commons License

a t_8: $R_H(t_8) = 0, R_H^{'}(t_8) < 0$ and $S(t) > 0, I_L(t) > 0, \ldots, R(t) > 0$ for $0 < t < t_8$ or there exists a t_9: $I_{AL}(t_9) = 0, I_{AL}^{'}(t_9) < 0$ and $(t) > 0, I_L(t) > 0, \ldots, R(t) > 0$ for $0 < t < t_9$ or there exists a t_{10}: $I_{CL}(t_{10}) = 0, I_{CL}^{'}(t_{10}) < 0$ and $S(t) > 0, I_L(t) > 0, \ldots, R(t) > 0$ for $0 < t < t_{10}$ or there exists a t_{11}: $I_{AT}(t_{11}) = 0, I_{AT}^{'}(t_{11}) < 0$ and $S(t) > 0, I_L(t) > 0, \ldots, R(t) > 0$ for $0 < t < t_{11}$ or there exists a t_{12}: $I_{CT}(t_{12}) = 0, I_{CT}^{'}(t_{12}) < 0$ and $S(t) > 0, I_L(t) > 0, \ldots, R(t) > 0$ for $0 < t < t_{12}$ or there exists a t_{13}: $R(t_{13}) = 0, R^{'}(t_{13}) < 0$ and $S(t) > 0, I_L(t) > 0, \ldots, R(t) > 0$ for $0 < t < t_{13}$. □

Considering differential equation one of model system (4), we get

$$\begin{aligned}\frac{dS(t_1)}{dt} &= \Lambda + \nu_1 R_H(t_1) + \nu_2 R_T(t_1) + \nu_3 R(t_1) + \pi I_A(t_1) \\ &\quad + \eta I_L(t_1) + \gamma I_{AL}(t_1) - (\lambda_T + \lambda_H + \mu) S(t_1), \\ &= \Lambda + \nu_1 R_H(t_1) + \nu_2 R_T(t_1) + \nu_3 R(t_1) + \pi I_A(t_1) \\ &\quad + \eta I_L(t_1) + \gamma I_{AL}(t_1) > 0,\end{aligned} \tag{6}$$

leading to a discrepancy; thus, $S(t)$ stays positive.

Considering differential equation two of model System (4), we get

$$\begin{aligned}\frac{dI_L(t_2)}{dt} &= \lambda_T S(t_2) + p_1 \pi I_{AL}(t_2) - (\theta + \eta + \mu + \lambda_H) I_L(t_2) \\ &= \lambda_T S(t_2) + p_1 \pi I_{AL}(t_2) > 0,\end{aligned} \tag{7}$$

leading to a discrepancy; thus, $I_L(t)$ stays positive.

Considering differential equation three of model System (4), we get

$$\begin{aligned}\frac{dI_T(t_3)}{dt} &= \theta I_L(t_3) - (\omega_1 + \rho + \mu + \sigma_1 + \lambda_H) I_T(t_3) \\ &= \theta I_L(t_3) > 0,\end{aligned} \tag{8}$$

leading to a discrepancy; thus, $I_T(t)$ stays positive.

Considering differential equation four of model System (4), we get

$$\begin{aligned}\frac{dH(t_4)}{dt} &= \rho I_T(t_4) - (\omega_2 + \mu + \sigma_2) H(t_4) \\ &= \rho I_T(t_4) > 0,\end{aligned} \tag{9}$$

leading to a discrepancy; thus, $H(t)$ stays positive.

Considering differential equation five of model System (4), we get

$$\begin{aligned}\frac{dR_T(t_5)}{dt} &= \omega_2 H(t_5) + \omega_1 I_T(t_5) - (\nu_2 + \mu) R_T(t_5) \\ &= \omega_2 H(t_5) + \omega_1 I_T(t_5) > 0,\end{aligned} \tag{10}$$

leading to a discrepancy; thus, $R_T(t)$ stays positive.

Considering differential equation six of model System (4), we get

$$\begin{aligned}\frac{dI_A(t_6)}{dt} &= \lambda_H S(t_6) + p_2 \eta I_{AL}(t_6) - (\pi + \alpha + \mu + \lambda_T) I_A(t_6) \\ &= \lambda_H S(t_6) + p_2 \eta I_{AL}(t_6) > 0,\end{aligned} \tag{11}$$

leading to a discrepancy; thus, $I_A(t)$ stays positive.

Considering differential equation seven of model System (4), we get

$$\begin{aligned}\frac{dI_C(t_7)}{dt} &= \alpha I_A(t_7) - (\psi + \mu + \delta + \lambda_T) I_C(t_7) \\ &= \alpha I_A(t_7) > 0,\end{aligned} \tag{12}$$

leading to a discrepancy; thus, $I_C(t)$ stays positive.

Considering differential equation eight of model System (4), we get

$$\begin{aligned}\frac{dR_H(t_8)}{dt} &= \psi I_C(t_8) - (\nu_1 + \mu) R_H(t_8) \\ &= \psi I_C(t_8) > 0,\end{aligned} \tag{13}$$

leading to a discrepancy; thus, $R_H(t)$ stays positive.

Considering differential equation nine of model System (4), we get

$$\begin{aligned}\frac{dI_{AL}(t_9)}{dt} &= \lambda_T I_A(t_9) + \lambda_H I_L(t_9) \\ &\quad - (\tau_1 + \mu + \beta_1 + \gamma + p_1 \pi + p_2 \eta) I_{AL}(t_9) \\ &= \lambda_T I_A(t_9) + \lambda_H I_L(t_9) > 0,\end{aligned} \tag{14}$$

leading to a discrepancy; thus, $I_{AL}(t)$ stays positive.

Considering differential equation ten of model System (4), we get

$$\begin{aligned}\frac{dI_{CL}(t_{10})}{dt} &= \beta_1 I_{AL}(t_{10}) + \lambda_T I_C(t_{10}) \\ &\quad - (r_1 + \tau_2 + \mu + \delta) I_{CL}(t_{10}) \\ &= \beta_1 I_{AL}(t_{10}) + \lambda_T I_C(t_{10}) > 0,\end{aligned} \tag{15}$$

leading to a discrepancy; thus, $I_{CL}(t)$ stays positive.

Considering differential equation 11 of model System (4), we get

$$\begin{aligned}\frac{dI_{AT}(t_{11})}{dt} &= \tau_1 I_{AL}(t_{11}) + \lambda_H I_T(t_{11}) \\ &\quad - (r_2 + \beta_2 + \mu + d_1) I_{AT}(t_{11}) \\ &= \tau_1 I_{AL}(t_{11}) + \lambda_H I_T(t_{11}) > 0,\end{aligned} \tag{16}$$

leading to a discrepancy; thus, $I_{AT}(t)$ stays positive.

Considering differential equation 12 of model System (4), we get

$$\begin{aligned}\frac{dI_{CT}(t_{12})}{dt} &= \tau_2 I_{CL}(t_{12}) + \beta_2 I_{AT}(t_{12}) \\ &\quad - (r_3 + \mu + d_2) I_{CT}(t_{12}) \\ &= \tau_2 I_{CL}(t_{12}) + \beta_2 I_{AT}(t_{12}) > 0,\end{aligned} \tag{17}$$

leading to a discrepancy; thus, $I_{CT}(t)$ stays positive.

Considering differential equation 13 of model System (4), we get

$$\begin{aligned}\frac{dR(t_{13})}{dt} &= r_1 I_{CL}(t_{13}) + r_2 I_{AT}(t_{13}) + r_3 I_{CT}(t_{13}) \\ &\quad - (\nu_3 + \mu) R(t_{13}) \\ &= r_1 I_{CL}(t_{13}) + r_2 I_{AT}(t_{13}) + r_3 I_{CT}(t_{13}) > 0,\end{aligned} \tag{18}$$

4185, 2026, 1, Downloaded from https://onlinelibrary.wiley.com/doi/10.1155/jama/8033235 by Readcube (Labtiva Inc.), Wiley Online Library on [12/11/2026]. See the Terms and Conditions (https://onlinelibrary.wiley.com/terms-and-conditions) on Wiley Online Library for rules of use; OA articles are governed by the applicable Creative Commons License

leading to a discrepancy; thus, $R(t)$ stays positive.

Therefore, in all cases, the solutions of the variables $S(t), I_L(t), I_T(t), H(t), R_T(t), I_A(t), I_C(t), \quad \backslash\backslash R_H(t), I_{AL}(t), I_{CL}(t), I_{AT}(t), I_{CT}(t)$ and $R(t)$ remain positive.

Theorem 2. *The region*

$$\Omega = (S(t), I_L(t), I_T(t), H(t), R_T(t), I_A(t), I_C(t), R_H(t), I_{AL}(t), I_{CL}(t), I_{AT}(t), I_{CT}(t), R(t)) \in \mathbb{R}_+^{13}: 0 \le N(t) \le \frac{\Lambda}{\mu}\Big\}, \tag{19}$$

is a positively invariant and attractive set with respect to the model.

Proof 2. Let

$$(S(t), I_L(t), I_T(t), H(t), R_T(t), I_A(t), I_C(t), R_H(t), I_{AL}(t), I_{CL}(t), I_{AT}(t), I_{CT}(t), R(t)) \in \mathbb{R}_+^{13}, \tag{20}$$

be a solution to System (4) chosen arbitrarily, subject to non-negative values as in Equation (5). □

By adding the equations in System (4) together, we obtain

$$\frac{dN}{dt} = \Lambda - \mu N - \eta I_L - \sigma_1 I_T - \sigma_2 H - \delta(I_C + I_{CL}) - d_1 I_{AT} - d_2 I_{CT}. \tag{21}$$

Since $I_L, I_T, H, I_A, I_C, I_{AL}, I_{CL}, IAT, I_{CT} \ge 0$ for $t \ge 0$, then Equation (21) simplifies to

$$\frac{dN}{dt} \le \Lambda - \mu N, \tag{22}$$

which we can rewrite as

$$\frac{dN}{dt} + \mu N \le \Lambda. \tag{23}$$

Now, solving inequality (23) subject to the initial conditions $N(t = 0) = N_0$, we obtain

$$Ne^{\mu t} \le \frac{\Lambda}{\mu} e^{\mu t} + N_0 - \frac{\Lambda}{\mu}. \tag{24}$$

Rearranging (24) leads to

$$N \le \frac{\Lambda}{\mu} + \left(N_0 - \frac{\Lambda}{\mu}\right) e^{-\mu t}. \tag{25}$$

Thus, we get

$$0 \le N(t) \le \frac{\Lambda}{\mu} + N_0 e^{-\mu t}. \tag{26}$$

Clearly, as $t \longrightarrow \infty$, we have

$$0 \le N(t) \le \frac{\Lambda}{\mu}. \tag{27}$$

This result implies that any feasible solution of the model system (4) that starts in the region Ω remains confined to that region for all time t. Consequently, region Ω is a biologically meaningful and trapping region, meaning it remains stable under the system's dynamics. Therefore, the model is both mathematically well-defined and biologically relevant.

Calculation of the effective reproduction numbers is carried out, by first gaining insights into the distinct behaviour of the TB-only and HCV-only submodels with treatment and thereafter the TB–HCV coinfection model with treatment.

By effective reproduction number, we mean the average number of secondary infections caused by a single infective, at a given susceptible fraction [41].

3.2 | TB-Only Sub Model

By ignoring all terms associated with HCV, the full model system (4) simplifies to the TB-only model. That is, $I_A(t) = I_C(t) = R_H(t) = I_{AL}\ (t) = I_{CL}(t) = I_{AT}(t) = I_{CT}(t) = R(t) = 0$.

Therefore, the TB-only submodel now becomes

$$\begin{aligned}
\frac{dS(t)}{dt} &= \Lambda + \eta I_L(t) + \nu_2 R_T(t) - (\lambda_T + \mu) S(t),\\
\frac{dI_L(t)}{dt} &= \lambda_T S(t) - (\theta + \eta + \mu) I_L(t),\\
\frac{dI_T(t)}{dt} &= \theta I_L(t) - (\omega_1 + \rho + \mu + \sigma_1) I_T(t),\\
\frac{dH(t)}{dt} &= \rho I_T(t) - (\omega_2 + \mu + \sigma_2) H(t),\\
\frac{dR_T(t)}{dt} &= \omega_1 I_T(t) + \omega_2 H(t) - (\nu_2 + \mu) R_T(t),
\end{aligned} \tag{28}$$

where,

$$\lambda_T(t) = \frac{\xi_1 q_1 (I_T(t) + \epsilon H(t))}{N_{TB}(t)}, \tag{29}$$

and

$$N_{TB}(t) = S(t) + I_L(t) + I_T(t) + H(t) + R_T(t). \tag{30}$$

The TB-free equilibrium point for the TB-only submodel is determined by assuming that there is no TB infection in the population. Thus, the TB-free equilibrium point for the TB-only submodel is given by

$$E_{TB}^o = (S, I_L, I_T, H, R_T) = \left(\frac{\Lambda}{\mu}, 0, 0, 0, 0\right). \tag{31}$$

The next generation matrix method [42, 43], is used to compute the effective reproduction number R_{TB} for the TB-only submodel with treatment.

The matrix representing the rate of new TB cases emerging in compartment i, F_i, specific to the TB-only submodel (28) is

$$F_i = \begin{bmatrix} \lambda_T S \\ 0 \\ 0 \end{bmatrix}. \tag{32}$$

The matrix, V_i, which represents the transfer rates between compartments i and all other compartments, is given by

$$V_i = \begin{bmatrix} (\eta + \mu + \theta) I_L \\ -\theta I_L + (\omega_1 + \rho + \mu + \sigma_1) I_T \\ -\rho I_T + (\omega_2 + \mu + \sigma_2) H \end{bmatrix}. \tag{33}$$

4185, 2026, 1, Downloaded from https://onlinelibrary.wiley.com/doi/10.1155/jama/8033235 by Readcube (Labtiva Inc.), Wiley Online Library on [12/11/2026]. See the Terms and Conditions (https://onlinelibrary.wiley.com/terms-and-conditions) on Wiley Online Library for rules of use; OA articles are governed by the applicable Creative Commons License

Thus, the TB induced effective reproduction number, R_{TB}, is calculated as

$$R_{TB} = \frac{\xi_1 q_1 \theta}{(\eta+\mu+\theta)(\omega_1+\rho+\mu+\sigma_1)}\left(1+\frac{\epsilon\rho}{(\omega_2+\mu+\sigma_2)}\right). \quad (34)$$

Lemma 1. *The TB infection-free equilibrium, E^0_{TB}, is locally asymptotically stable if $R_{TB} < 1$ and unstable otherwise.*

Proof 3. The Jacobian matrix of the TB-only submodel (28) is given by

$$J(E_{TB}) = \begin{bmatrix} -\left(\xi_1 q_1 \frac{(I_T+\epsilon H)}{N_{TB}}+\mu\right) & \eta & -\xi_1 q_1 & \xi_1 q_1 \epsilon & \nu_2 \\ \xi_1 q_1 \frac{(I_T+\epsilon H)}{N_{TB}} & -\kappa_1 & \xi_1 q_1 & \xi_1 q_1 \epsilon & 0 \\ 0 & \theta & -\kappa_2 & 0 & 0 \\ 0 & \rho & 0 & -k_3 & 0 \\ 0 & 0 & \omega_1 & \omega_2 & -(\nu_2+\mu) \end{bmatrix}, \quad (35)$$

where

$$\kappa_1 = \theta+\eta+\mu, \kappa_2 = \omega_1+\rho+\mu+\sigma_1, \kappa_3 = \omega_2+\mu+\sigma_2. \quad (36)$$

□

At TB infection free equilibrium point, $E^0_{TB} = (\Lambda/\mu, 0, 0, 0, 0)$, the Jacobian matrix becomes:

$$J(E_{TB}) = \begin{bmatrix} -\mu & \eta & -\xi_1 q_1 & \xi_1 q_1 \epsilon & \nu_2 \\ 0 & -k_1 & \xi_1 q_1 & \xi_1 q_1 \epsilon & 0 \\ 0 & \theta & -\kappa_2 & 0 & 0 \\ 0 & \rho & 0 & -\kappa_3 & 0 \\ 0 & 0 & \omega_1 & \omega_2 & -(\nu_2+\mu) \end{bmatrix}. \quad (37)$$

However, $J(E^0_{TB})$ can be expressed in the form

$$J(E^0_{TB}) = \begin{bmatrix} J_{11} & J_{12} \\ J_{21} & J_{22} \end{bmatrix}, \quad (38)$$

where

$$J_{11} = \begin{bmatrix} -\mu & \eta & -\xi_1 q_1 \\ 0 & -\kappa_1 & \xi_1 q_1 \\ 0 & \theta & -\kappa_2 \end{bmatrix}, J_{12} = \begin{bmatrix} -\xi_1 q_1 \epsilon & \nu_2 \\ \xi_1 q_1 \epsilon & 0 \\ 0 & 0 \end{bmatrix}, \quad (39)$$
$$J_{21} = \begin{bmatrix} 0 & \rho & 0 \\ 0 & 0 & \omega_1 \end{bmatrix} \text{and} J_{22} = \begin{bmatrix} -\kappa_3 & 0 \\ \omega_2 & -(\nu_2+\mu) \end{bmatrix}.$$

An essential and requisite condition for local asymptotic stability of the disease-free equilibrium is that all the eigenvalues of submatrices J_{11} and J_{22} have negative real parts [16, 39].

For the eigenvalues of submatrix J_{22}, we have

$$\det(J_{22} - \lambda I) = 0, \quad (40)$$

where I is a 2×2 matrix. Therefore,

$$\det\begin{bmatrix} -k_3-\lambda & 0 \\ \omega_2 & -(\nu_2+\mu)-\lambda \end{bmatrix} = 0. \quad (41)$$

On solving Equation (41) for the eigenvalues, we get

$$\lambda_1 = -\kappa_3 \text{ and } \lambda_2 = -(\nu_2+\mu). \quad (42)$$

Thus, the eigenvalues of J_{22} are $-\kappa_3$ and $-(\nu_2+\mu)$ which are both negative.

Now, the eigenvalues of J_{11} are calculated as follows:

$$\det(J_{11} - \lambda I) = 0, \quad (43)$$

$$\det\begin{bmatrix} -\mu-\lambda & \eta & -\xi_1 q_1 \\ 0 & -\kappa_1-\lambda & \xi_1 q_1 \\ 0 & \theta & -\kappa_2-\lambda \end{bmatrix} = 0, \quad (44)$$

On solving Equation (44) for the eigenvalues, we get

$$\lambda_3 = -\mu, \lambda_4 = \frac{-(\kappa_1+\kappa_2) - \sqrt{(\kappa_1+\kappa_2)^2 - 4(\kappa_1\kappa_2 - \theta\xi_1 q_1)}}{2},$$
$$\lambda_5 = \frac{-(\kappa_1+\kappa_2) + \sqrt{(\kappa_1+\kappa_2)^2 - 4(\kappa_1\kappa_2 - \theta\xi_1 q_1)}}{2}. \quad (45)$$

For λ_4 and λ_5 to be negative, then

$$-(\kappa_1+\kappa_2) \pm \sqrt{(\kappa_1+\kappa_2)^2 - 4(\kappa_1\kappa_2 - \theta\xi_1 q_1)} < 0. \quad (46)$$

Re-arranging inequality (46), we get

$$(\kappa_1+\kappa_2)^2 < (\kappa_1+\kappa_2)^2 - 4(\kappa_1\kappa_2 - \theta\xi_1 q_1). \quad (47)$$

On simplifying inequality (47), we have

$$\frac{\theta\xi_1 q_1}{\kappa_1\kappa_2} < 1. \quad (48)$$

Now, from

$$R_{TB} = \frac{\xi_1 q_1 \theta}{\kappa_1\kappa_2}\left(\frac{\kappa_3+\epsilon\rho}{\kappa_3}\right). \quad (49)$$

Re-arranging Equation (49), yields

$$\frac{\theta\xi_1 q_1}{\kappa_1\kappa_2} = \frac{\kappa_3 R_{TB}}{\kappa_3+\epsilon\rho}. \quad (50)$$

Thus, inequality (48) can be re-written as

$$\frac{\kappa_3 R_{TB}}{\kappa_3+\epsilon\rho} < 1. \quad (51)$$

Therefore, λ_4 and λ_5 are negative eigenvalues if inequality (51) is satisfied. Hence, the TB infection-free equilibrium E^0_{TB}, is locally asymptotically stable if $R_{TB} < 1$ and unstable otherwise. This suggests that in the event that a small group of TB-infected persons enter the population, the system will eventually return to the TB-free equilibrium over time.

4185, 2026, 1, Downloaded from https://onlinelibrary.wiley.com/doi/10.1155/jama/8033235 by Readcube (Labtiva Inc.), Wiley Online Library on [12/11/2026]. See the Terms and Conditions (https://onlinelibrary.wiley.com/terms-and-conditions) on Wiley Online Library for rules of use; OA articles are governed by the applicable Creative Commons License

3.2.1 | Global Stability of TB Infection-Free Equilibrium for TB-Only Sub Model

The global behaviour of TB-only sub-model (28) is analysed by applying the approach by Castillo-Chavez et al. [44] as also applied by [39, 45].

Rewriting the TB-only submodel (28) in the form

$$\begin{aligned}\frac{dX_{TB}}{dt} &= F(X_{TB}, Z_{TB}),\\ \frac{dZ_{TB}}{dt} &= G(X_{TB}, Z_{TB}), G(X_{TB}, 0) = 0,\end{aligned} \tag{52}$$

where $X_{TB} = (S)$ and $Z_{TB} = (I_L, I_T, H, R_T)$, with $X_{TB} \in \mathbb{R}_+$ denoting (its components) the number of uninfected humans and $Z_{TB} \in \mathbb{R}_+^4$ with components defining the number of individuals infected with TB including those ones on treatment. Let $E_{TB}^0 = (X_{TB}^0, 0) = (\Lambda/\mu, 0, 0, 0, 0)$ denote the TB infection free equilibrium of system (52).

Theorem 3. *The fixed point $E_{TB}^0 = (X_{TB}, 0)$ is a globally asymptotic stable equilibrium of system (52) provided $R_{TB} < 1$ and that the following conditions are satisfied.*

$$\begin{aligned}&D1\text{: For } \frac{dX_{TB}}{dt} = F(X_{TB}, 0), X_{TB}^0\\ &\quad \text{is globally asymptotically stable,}\\ &D2\text{: } G(X_{TB}, Z_{TB}) = MZ_{TB} - \widehat{G}(X_{TB}, Z_{TB}),\\ &\quad \widehat{G}(X_{TB}, Z_{TB}) \geq 0, \quad \text{for} (X_{TB}, Z_{TB}) \in \Omega_{TB},\end{aligned} \tag{53}$$

where $M = \partial/\partial Z_{TB} G(X_{TB}^0, 0)$ is a Metzler matrix and Ω_{TB} is the invariant region in which the model makes biological sense.

Proof 4. By the result of Lemma 1, local asymptotic stability of E_{TB}^0 is guaranteed if $R_{TB} < 1$, implying a stable equilibrium. □

Regarding the first condition ($D1$) which pertains to the global asymptotic stability of X_{TB}^0, we obtain

$$F(X_{TB}, Z_{TB}) = \begin{bmatrix} \Lambda + \eta I_L + \nu_2 R_T - (\lambda_T + \mu)S \\ 0 \end{bmatrix}, \tag{54}$$

and

$$\frac{dX_{TB}}{dt} = F(X_{TB}, 0) = \Lambda - \mu S, \tag{55}$$

which takes the form of a linear differential equation. Solving Equation (55) yields

$$S(t) = \frac{\Lambda}{\mu} - \frac{\Lambda}{\mu} e^{-\mu t} + S(0) e^{-\mu t}. \tag{56}$$

As t increases without bound, $S(t) \longrightarrow \Lambda/\mu$ irrespective of the initial conditions $S(0)$. Thus, convergence in Ω_{TB}, necessarily implies condition ($D1$) holds true.

With regard to the second requirement ($D2$), consider

$$\begin{aligned} G_{TB}(X_{TB}, Z_{TB}) &= \begin{bmatrix} \lambda_T S - \kappa_1 I_L \\ \theta I_L - \kappa_2 I_T \\ \rho I_T - \kappa_3 H \\ \omega_1 I_T + \omega_2 H - (\nu_2 + \mu) R_T \end{bmatrix}\\ &= \begin{bmatrix} \xi_1 q_1 (I_T + \epsilon H)\dfrac{S}{N_{TB}} - \kappa_1 I_L \\ \theta I_L - \kappa_2 I_T \\ \rho I_T - \kappa_3 H \\ \omega_1 I_T + \omega_2 H - (\nu_2 + \mu) R_T \end{bmatrix}, \end{aligned} \tag{57}$$

and

$$M = \frac{\partial}{\partial Z_{TB}} G_{TB}(X_{TB}^0, 0) = \begin{bmatrix} -\kappa_1 & \xi_1 q_1 \dfrac{S}{N_{TB}} & \xi_1 q_1 \epsilon \dfrac{S}{N_{TB}} & 0 \\ \theta & -\kappa_2 & 0 & 0 \\ 0 & \rho & -\kappa_3 & 0 \\ 0 & \omega_1 & \omega_2 & -(\nu_2 + \mu) \end{bmatrix}. \tag{58}$$

Now, at E_{TB}^0

$$M = \frac{\partial}{\partial Z_{TB}} G_{TB}(X_{TB}^0, 0) = \begin{bmatrix} -\kappa_1 & \xi_1 q_1 & \xi_1 q_1 \epsilon & 0 \\ \theta & -\kappa_2 & 0 & 0 \\ 0 & \rho & -\kappa_3 & 0 \\ 0 & \omega_1 & \omega_2 & -(\nu_2 + \mu) \end{bmatrix}. \tag{59}$$

But

$$\widehat{G_{TB}}(X_{TB}, Z_{TB}) = MZ_{TB} - G_{TB}(X_{TB}, Z_{TB}). \tag{60}$$

Substituting Equations (58)–(60), and on simplifying, we have

$$\widehat{G_{TB}}(X_{TB}, Z_{TB}) = \begin{bmatrix} \xi_1 q_1 I_T \left(1 - \dfrac{S}{N_{TB}}\right) + \xi_1 q_1 \epsilon H \left(1 - \dfrac{S}{N_{TB}}\right) \\ 0 \\ 0 \\ 0 \end{bmatrix}. \tag{61}$$

Given that $0 < S \leq N_{TB}$, it follows easily that $\widehat{G_{TB}}(X_{TB}, Z_{TB}) \geq 0$. Additionally, matrix M is a Metzler matrix with all off-diagonal entries being positive or zero. It follows that, E_{TB}^0 is globally asymptotically stable when $R_{TB} < 1$. This means that irrespective of the number of TB infectives introduced into the population, TB will gradually phase out.

4185, 2026, 1, Downloaded from https://onlinelibrary.wiley.com/doi/10.1155/jama/8033235 by Readcube (Labtiva Inc.), Wiley Online Library on [12/11/2026]. See the Terms and Conditions (https://onlinelibrary.wiley.com/terms-and-conditions) on Wiley Online Library for rules of use; OA articles are governed by the applicable Creative Commons License

3.3 | The Endemic Equilibrium Point, E^*_{TB}

The TB endemic equilibrium, E^*_{TB}, occurs when TB infections persists in the population. Now, by equating the derivatives of system (28) in the TB-only submodel to zero, we can solve for the endemic equilibrium E^*_{TB} as

$$E^*_{TB} = \left(\frac{\kappa_1\kappa_2\kappa_3 N^*_{TB}}{\xi_1 q_1\theta(\kappa_3+\epsilon\rho)}, \frac{\kappa_2\kappa_3\left(\Lambda-\mu N^*_{TB}\right)}{\theta(\sigma_1\kappa_3+\sigma_2\rho)}, \frac{\kappa_3\left(\Lambda-\mu N^*_{TB}\right)}{(\sigma_1\kappa_3+\sigma_2\rho)}, \frac{\rho\left(\Lambda-\mu N^*_{TB}\right)}{(\sigma_1\kappa_3+\sigma_2\rho)}, \frac{\left(\Lambda-\mu N^*_{TB}\right)(\omega_2\rho+\omega_1\kappa_3)}{(\nu_2+\mu)(\sigma_1\kappa_3+\sigma_2\rho)}\right). \tag{62}$$

Lemma 2. *The TB-only submodel (28) has a unique endemic equilibrium point if $R_{TB} > 1$.*

Proof 5. If the disease is endemic in the population, then $dI_L/dt > 0$, $dI_T/dt > 0$ and $dH/dt > 0$, that is

$$\xi_1 q_1(I_T+\epsilon H)\frac{S}{N_{TB}} - \kappa_1 I_L > 0, \tag{63}$$

$$\theta I_L - \kappa_2 I_T > 0, \tag{64}$$

$$\rho I_T - \kappa_3 H > 0. \tag{65}$$

□

From inequality (63), we have

$$\kappa_1 I_L < \xi_1 q_1(I_T+\epsilon H)\frac{S}{N_{TB}}. \tag{66}$$

Using the fact that $S/N_{TB} \le 1$, inequality (66) becomes

$$I_L < \frac{\xi_1 q_1}{\kappa_1}(I_T+\epsilon H). \tag{67}$$

From inequality (65), we have

$$H < \frac{\rho I_T}{\kappa_3}. \tag{68}$$

Substituting H into inequality (67), we get

$$I_L < \frac{\xi_1 q_1}{\kappa_1}\left(1+\frac{\epsilon\rho}{\kappa_3}\right)I_T. \tag{69}$$

Now, re-arranging inequality (64), we have

$$I_T < \frac{\theta I_L}{\kappa_2}. \tag{70}$$

Substituting I_T into inequality (69) and simplifying, we get

$$1 < \frac{\xi_1 q_1\theta}{\kappa_1\kappa_2}\left(1+\frac{\epsilon\rho}{\kappa_3}\right). \tag{71}$$

Thus, $R_{TB} > 1$.

Hence, a unique endemic equilibrium point E^*_{TB} exists when $R_{TB} > 1$.

Lemma 3. *If $R_{TB} > 1$, the TB endemic equilibrium E^*_{TB} is locally stable, otherwise, it is unstable.*

Proof 6. We study the local stability of the TB endemic equilibrium by applying the Routh-Hurwitz criterion. □

The Jacobian matrix of TB-only submodel is given by

$$J(E_{TB}) = \begin{bmatrix} -\left(\xi_1 q_1\frac{\left(I^*_T+\epsilon H^*\right)}{N^*_{TB}}+\mu\right) & \eta & -\xi_1 q_1 & -\xi_1 q_1\epsilon & \nu_2 \\ \xi_1 q_1\frac{\left(I^*_T+\epsilon H^*\right)}{N^*_{TB}} & -\kappa_1 & \xi_1 q_1 & \xi_1 q_1\epsilon & 0 \\ 0 & \theta & -\kappa_2 & 0 & 0 \\ 0 & \rho & 0 & -\kappa_3 & 0 \\ 0 & 0 & \omega_1 & \omega_2 & -(\nu_2+\mu) \end{bmatrix}. \tag{72}$$

At the TB endemic equilibrium, the Jacobian matrix $J(E_{TB})$ becomes

$$J\left(E^*_{TB}\right) = \begin{bmatrix} -(z^*+\mu) & \eta & -\xi_1 q_1 & -\xi_1 q_1\epsilon & \nu_2 \\ z^* & -\kappa_1 & \xi_1 q_1 & \xi_1 q_1\epsilon & 0 \\ 0 & \theta & -\kappa_2 & 0 & 0 \\ 0 & \rho & 0 & -\kappa_3 & 0 \\ 0 & 0 & \omega_1 & \omega_2 & -(\nu_2+\mu) \end{bmatrix}, \tag{73}$$

where

$$z^* = \xi_1 q_1\frac{\left(I^*_T+\epsilon H^*\right)}{N^*_{TB}}, \tag{74}$$

denotes the force of TB infection at the equilibrium where the disease persists.

The characteristic polynomial of the Jacobian matrix $J(E^*_{TB})$ is obtained as

$$P(\lambda) = \det\left(\lambda I - J\left(E^*_{TB}\right)\right) = \lambda^5 + e_1\lambda^4 + e_2\lambda^3 + e_3\lambda^2 + e_4\lambda + e_5, \tag{75}$$

where I is a 5×5 identity matrix and

$$\begin{aligned}
e_1 &= \kappa_1+\kappa_2+\kappa_3+z^*+\mu+\nu_2,\\
e_2 &= \kappa_2\kappa_3+(\kappa_1+z^*+\mu)(\kappa_2+\kappa_3)+\kappa_1(z^*+\mu)\\
&\quad+\nu_2(\kappa_2+\kappa_3)+\nu_2(\kappa_1+z^*+\mu)-\xi_1 q_1\epsilon\rho-\xi_1 q_1\theta-\eta z^*,\\
e_3 &= \kappa_2\kappa_3(\kappa_1+z^*+\mu)+(\kappa_1(\kappa_2+\kappa_3)(z^*+\mu)+\kappa_2\kappa_3\nu_2\\
&\quad+\nu_2(\kappa_1+z^*+\mu)(\kappa_2+\kappa_3)+\kappa_1\nu_2(z^*+\mu)-\xi_1 q_1 z^*\theta\\
&\quad-\xi_1 q_1\epsilon\rho(z^*+\mu+\kappa_2)-\xi_1 q_1\epsilon\rho\nu_2-\xi_1 q_1\theta(z^*+\mu+\kappa_3)\\
&\quad-\xi_1 q_1\theta\nu_2-\eta z^*(\kappa_2+\kappa_3)-\eta z^*\nu_2-\xi_1 q_1\epsilon z^*\rho,\\
e_4 &= \kappa_1\kappa_2\kappa_3(z^*+\mu)+\kappa_2\kappa_3\nu_2(\kappa_1+z^*+\mu)\\
&\quad+\kappa_1\nu_2(\kappa_2+\kappa_3)(z^*+\mu)+\xi_1 q_1 z^*\theta(\kappa_3+\nu_2)\\
&\quad-\xi_1^2 q_1^2\epsilon\rho\kappa_2-\xi_1 q_1\epsilon\rho\nu_2(z^*+\mu+\kappa_2)-\xi_1^2 q_1^2\epsilon\theta\kappa_3\\
&\quad-\xi_1 q_1\theta\nu_2(z^*+\mu+\kappa_3)-\nu_2\omega_2\rho z^*-\nu_2\omega_2 z^*\theta\\
&\quad-\eta z^*\kappa_2\kappa_3-\eta z^*\nu_2(\kappa_2+\kappa_3)-\xi_1 q_1\epsilon z^*\rho(\kappa_1+\nu_2),\\
e_5 &= \kappa_1\kappa_2\kappa_3\nu_2(z^*+\mu)-\xi_1 q_1 z^*\theta\nu_2\kappa_3-\xi_1^2 q_1^2\epsilon\rho\nu_2\kappa_2\\
&\quad-\xi_1^2 q_1^2\epsilon\theta\nu_2\kappa_3-\nu_2\omega_2\rho z^*\kappa_2-\omega_2\nu_2 z^*\theta\kappa_2\\
&\quad-\eta z^*\nu_2\kappa_2\kappa_3-\xi_1 q_1\epsilon z^*\rho\kappa_2\nu_2.
\end{aligned} \tag{76}$$

The TB endemic equilibrium is locally asymptotically stable if and only if the Routh-Hurwitz criterion is satisfied. The criterion

4185, 2026, 1, Downloaded from https://onlinelibrary.wiley.com/doi/10.1155/jama/8033235 by Readcube (Labtiva Inc.), Wiley Online Library on [12/11/2026]. See the Terms and Conditions (https://onlinelibrary.wiley.com/terms-and-conditions) on Wiley Online Library for rules of use; OA articles are governed by the applicable Creative Commons License

states that the polynomial, $P(\lambda)$, has all roots with negative real parts if and only if the determinants of all Hurwitz matrices, H, are positive, that is $\det H_i > 0$, $i = 1, 2, 3, 4, 5$ [46]. According to [46], for a characteristic polynomial of degree five, the determinants are given by

$$\begin{aligned} H_1 &= e_1 > 0, \\ H_2 &= e_1e_2 - e_3 > 0, \\ H_3 &= e_1e_2e_3 + e_1e_3 + e_1e_5 - e_1e_4 - e_3 > 0, \\ H_4 &= (e_3e_4 - e_2e_5)(e_1e_2 - e_3) - (e_1e_4 - e_5) > 0, \\ H_5 &= e_5H_4 > 0. \end{aligned} \tag{77}$$

Now, when the determinants in (77) are satisfied, then a conclusion can be made that the TB endemic equilibrium is locally asymptotically stable.

3.3.1 | Global Stability of TB Endemic Equilibrium for TB-Only Submodel

In this subsection, we investigate the global stability of the TB endemic equilibrium, E^*_{TB}.

Lemma 4. *If $R_{TB} > 1$, then the TB endemic equilibrium, E^*_{TB}, of TB-only submodel system is globally asymptotically stable and unstable otherwise.*

Proof 7. To investigate the global stability of, E^*_{TB}, the Lyapunov function $L = L(S, I_L, I_T, H, R_T)$ is constructed as

$$\begin{aligned} L = {} & U_1\left(\left(S - S^* - S^*In\left(\frac{S}{S^*}\right)\right) + U_2\left(I_L - I_L^* - I_L^*In\left(\frac{I_L}{I_L^*}\right)\right)\right. \\ & + U_3\left(I_T - I_T^* - I_T^*In\left(\frac{I_T}{I_T^*}\right)\right) + U_4\left(H - H^* - H^*In\left(\frac{H}{H^*}\right)\right) \\ & \left. + U_5\left(R_T - R_T^* - R_T^*In\left(\frac{R_T}{R_T^*}\right)\right)\right), \end{aligned} \tag{78}$$

where $U_1, U_2, \ldots, U_5$ are positive constants. □

The time derivative of the Lyapunov function is given by

$$\begin{aligned} \frac{dL}{dt} = {} & U_1\left(1 - \frac{S^*}{S}\right)\frac{dS}{dt} + U_2\left(1 - \frac{I_L^*}{I_L}\right)\frac{dI_L}{dt} + U_3\left(1 - \frac{I_T^*}{I_T}\right)\frac{dI_T}{dt} \\ & + U_4\left(1 - \frac{H^*}{H}\right)\frac{dH}{dt} + U_5\left(1 - \frac{R_T^*}{R_T}\right)\frac{dR_T}{dt} \\ = {} & U_1\left(1 - \frac{S^*}{S}\right)\left(\Lambda + \eta I_L + \nu_2 R_T - \xi_1 q_1 \frac{(I_T + \epsilon H)}{N_{TB}} S\right. \\ & \left. - \mu S\right) + U_2\left(1 - \frac{I_L^*}{I_L}\right)\left(\xi_1 q_1 \frac{(I_T + \epsilon H)}{N_{TB}} S - \kappa_1 I_L\right) \\ & + U_3\left(1 - \frac{I_T^*}{I_T}\right)(\theta I_L - \kappa_2 I_T) + U_4\left(1 - \frac{H^*}{H}\right)(\rho I_T - \kappa_3 H) \\ & + U_5\left(1 - \frac{R_T^*}{R_T}\right)(\omega_1 I_T + \omega_2 H - \kappa_4 R_T), \end{aligned} \tag{79}$$

where $\kappa_4 = \nu + \mu$.

At the equilibrium point where TB becomes endemic, we observe that

$$\begin{aligned} \Lambda &= \xi_1 q_1 \frac{(I_T^* + \epsilon H^*)}{N_{TB}^*} S^* + \mu S^* - \eta I_L^* - \nu_2 R_T^*, \\ \kappa_1 &= \xi_1 q_1 \frac{(I_T^* + \epsilon H^*)}{N_{TB}^* I_L^*} S^*, \\ \kappa_2 &= \frac{\theta I_L^*}{I_T^*}, \\ \kappa_3 &= \frac{\rho I_L^*}{H^*}, \\ \kappa_4 &= \frac{(\omega_1 I_T^* + \omega_2 H^*)}{R_T^*}. \end{aligned} \tag{80}$$

Now, substituting Equation (80) into (79), we get

$$\begin{aligned} \frac{dL}{dt} = {} & U_1\left(1 - \frac{S^*}{S}\right)\left(\xi_1 q_1 \frac{(I_T^* + \epsilon H^*)}{N_{TB}^*} S^* + \mu S^* - \eta I_L^*\right. \\ & \left. - \nu_2 R_T^* + \eta I_L + \nu_2 R_T - \xi_1 q_1 \frac{(I_T + \epsilon H)}{N_{TB}} S - \mu S\right) \\ & + U_2\left(1 - \frac{I_L^*}{I_L}\right)\left(\xi_1 q_1 \frac{(I_T + \epsilon H)}{N_{TB}} S - \xi_1 q_1 \frac{(I_T^* + \epsilon H^*)}{N_{TB}^* I_L^*} S^* I_L\right) \\ & + U_3\left(1 - \frac{I_T^*}{I_T}\right)\left(\theta I_L - \frac{\theta I_L^*}{I_T^*} I_T\right) \\ & + U_4\left(1 - \frac{H^*}{H}\right)\left(\rho I_T - \frac{\rho I_L^*}{H^*} H\right) \\ & + U_5\left(1 - \frac{R_T^*}{R_T}\right)\left(\omega_1 I_T + \omega_2 H - \frac{(\omega_1 I_T^* + \omega_2 H^*)}{R_T^*} R_T\right). \end{aligned} \tag{81}$$

Expanding and reorganising the terms, we can separate them into positive and negative parts, giving:

$$\frac{dL}{dt} = -X + Y, \tag{82}$$

where

4185, 2026, 1, Downloaded from https://onlinelibrary.wiley.com/doi/10.1155/jama/8033235 by Readcube (Labtiva Inc.), Wiley Online Library on [12/11/2026]. See the Terms and Conditions (https://onlinelibrary.wiley.com/terms-and-conditions) on Wiley Online Library for rules of use; OA articles are governed by the applicable Creative Commons License

$$
\begin{aligned}
X = {} & \frac{U_1\xi_1 q_1 I_T S}{N_{TB}} + \frac{U_1\xi_1 q_1 \epsilon H S}{N_{TB}} + U_1\eta I_L^* + U_1\mu S \\
& + \frac{U_1\xi_1 q_1 I_T^* S^*}{N_{TB}^*}\frac{S^*}{S} + \frac{U_1\xi_1 q_1 \epsilon H S^*}{N_{TB}^*}\frac{S^*}{S} + U_1\mu S^*\frac{S^*}{S} \\
& + U_1\eta I_L\frac{S^*}{S} + U_1\nu_2 R_T\frac{S^*}{S} + \frac{U_1\xi_1 q_1 \epsilon H S^*}{N_{TB}} \\
& + \frac{U_2\xi_1 q_1 I_T^* S^*}{N_{TB}^*}\frac{I_L}{I_L^*} + \frac{U_2\xi_1 q_1 \epsilon H^* S^*}{N_{TB}^*}\frac{I_L}{I_L^*} + \frac{U_2\xi_1 q_1 I_T S}{N_{TB}}\frac{I_L^*}{I_L} \\
& + \frac{U_2\xi_1 q_1 \epsilon H S}{N_{TB}}\frac{I_L^*}{I_L} + U_3\theta I_L^*\frac{I_T}{I_T^*} + U_3\theta I_L^*\frac{I_T^*}{I_T} + U_4\rho I_L^*\frac{H}{H^*} \\
& + U_4\rho I_T\frac{H^*}{H} + U_5\omega_1 I_T^*\frac{R_T}{R_T^*} + U_5\omega_2 H\frac{R_T}{R_T^*} \\
& + U_5\omega_1 I_T\frac{R_T^*}{R_T} + U_5\omega_2 H\frac{R_T^*}{R_T},
\end{aligned} \tag{83}
$$

and

$$
\begin{aligned}
Y = {} & \frac{U_1\xi_1 q_1 I_T^* S^*}{N_{TB}^*} + \frac{U_1\xi_1 q_1 \epsilon H S^*}{N_{TB}^*} + U_1\mu S^* + U_1\eta I_L \\
& + U_1\nu_2 R_T + U_1\eta I_L^*\frac{S^*}{S} + U_1\nu_2 R_T^*\frac{S^*}{S} + \frac{U_1\xi_1 q_1 I_T S^*}{N_{TB}} \\
& + U_1\mu S^* + \frac{U_2\xi_1 q_1 I_T S}{N_{TB}} + \frac{U_2\xi_1 q_1 \epsilon H S}{N_{TB}} + \frac{U_2\xi_1 q_1 I_T^* S^*}{N_{TB}^*} \\
& + \frac{U_2\xi_1 q_1 \epsilon H^* S^*}{N_{TB}^*} + U_3\theta I_L + U_3\theta I_L^* + U_4\rho I_L + U_4\rho I_L^* \\
& + U_5\omega_1 I_T + U_5\omega_2 H + U_5\omega_1 I_T^* + U_5\omega_2 H^*.
\end{aligned} \tag{84}
$$

Hence, $dL/dt \le 0$ when $Y < X$; and $dL/dt = 0$ when $S = S^*, I_L = I^*L, I_T = I_T^*, H = H^*$ and $R_T = R_T^*$. Therefore, the largest invariant set $(S, I_L, I_T, H, R_T) \in \Omega$ such that $dL/dt = 0$ is the singleton (E_{TB}^*), E_{TB}^* is the TB endemic equilibrium for TB-only submodel system. According to Lasalle's invariant principle [47], the global asymptotic stability of E_{TB}^* is guaranteed when $Y < X$.

3.4 | The HCV-Only Submodel

The HCV-only submodel is derived by setting all the variables concerning TB infection to zero; that is, $I_L(t) = I_T(t) = H(t) = R_T(t) = I_{AL}(t) = I_{CL}\ \ (t) = I_{AT}(t) = I_{CT}(t) = R(t) = 0$. Then, the HCV-only submodel is as in Equation (85).

$$
\begin{aligned}
\frac{dS}{dt} &= \Lambda + \pi I_A + \nu_1 R_H - \lambda_H S - \mu S, \\
\frac{dI_A}{dt} &= \lambda_H S - (\pi + \alpha + \mu) I_A, \\
\frac{dI_C}{dt} &= \alpha I_A - (\psi + \mu + \delta) I_C, \\
\frac{dR_H}{dt} &= \psi I_C - (\mu + \nu_1) R_H,
\end{aligned} \tag{85}
$$

where

$$
\lambda_H = \xi_2 q_2 \frac{(\phi I_A + I_C)}{N_{HCV}}, \tag{86}
$$

and

$$
N_{HCV} = S + I_A + I_C + R_H. \tag{87}
$$

The HCV infection-free equilibrium is calculated by modelling a scenario where HCV has been entirely eliminated from the population. Consequently, the equilibrium point with no HCV infection in the HCV-only submodel is defined by

$$
E_{HCV}^0 = \left(S^0, I_A^0, I_C^0, R_H^0\right) = \left(\frac{\Lambda}{\mu}, 0, 0, 0\right). \tag{88}
$$

Lemma 5. *The effective reproduction number for HCV-only submodel (85) is*

$$
R_{HCV} = \frac{\xi_2 q_2(\phi(\psi + \mu + \delta) + \alpha)}{(\pi + \alpha + \mu)(\psi + \mu + \delta)}. \tag{89}
$$

Proof 8. To compute the effective reproduction number, R_{HCV}, the next generation matrix technique is employed [42, 48]. □

The matrix for the rate of appearance of new HCV infections in compartment i, F_i, for the HCV-only submodel (85) is given by

$$
F_i = \begin{bmatrix} \lambda_H S \\ 0 \\ 0 \end{bmatrix}. \tag{90}
$$

The rate of exchange between compartment i and other compartments through all processes is represented by V_i and given by

$$
V_i = \begin{bmatrix} (\pi + \alpha + \mu) I_A \\ -\alpha I_A + (\psi + \mu + \delta) I_C \\ -\psi I_C + (\mu + \nu_1) R_H \end{bmatrix}. \tag{91}
$$

Now, the Jacobian matrix, F_{HCV}, of the new HCV infections in compartment i at HCV infection free equilibrium point, is given by

$$
F_{HCV} = \begin{bmatrix} \xi_2 q_2 \phi & \xi_2 q_2 & 0 \\ 0 & 0 & 0 \\ 0 & 0 & 0 \end{bmatrix}. \tag{92}
$$

At the disease-free equilibrium, the Jacobian matrix, V_{HCV}, corresponding to the rate of exchange between compartment i through all processes is given by

$$
V_{HCV} = \begin{bmatrix} (\pi + \alpha + \mu) & 0 & 0 \\ -\alpha & (\psi + \mu + \delta) & 0 \\ 0 & -\psi & (\mu + \nu_1) \end{bmatrix}, \tag{93}
$$

and

4185, 2026, 1, Downloaded from https://onlinelibrary.wiley.com/doi/10.1155/jama/8033235 by Readcube (Labtiva Inc.), Wiley Online Library on [12/11/2026]. See the Terms and Conditions (https://onlinelibrary.wiley.com/terms-and-conditions) on Wiley Online Library for rules of use; OA articles are governed by the applicable Creative Commons License

$$V_{HCV}^{-1} = \begin{bmatrix} \frac{1}{(\pi+\alpha+\mu)} & 0 & 0 \\ \frac{\alpha}{(\pi+\alpha+\mu)(\psi+\mu+\delta)} & \frac{1}{(\psi+\mu+\delta)} & 0 \\ \frac{\alpha\psi}{(\pi+\alpha+\mu)(\psi+\mu+\delta)(\mu+\nu_1)} & \frac{\psi}{(\psi+\mu+\delta)(\mu+\nu_1)} & \frac{1}{(\mu+\nu_1)} \end{bmatrix}. \tag{94}$$

Now,

$$F_{HCV}V_{HCV}^{-1} = \begin{bmatrix} \frac{\xi_2 q_2 \phi}{(\pi+\alpha+\mu)} + \frac{\xi_2 q_2 \alpha}{(\pi+\alpha+\mu)(\psi+\mu+\delta)} & \frac{\xi_2 q_2}{(\psi+\mu+\delta)} & 0 \\ 0 & 0 & 0 \\ 0 & 0 & 0 \end{bmatrix}. \tag{95}$$

For the eigenvalues, λ, we solve the equation

$$\det\left(\lambda I - F_{HCV}V_{HCV}^{-1}\right) = 0,$$

$$\det\begin{bmatrix} \lambda - \frac{\xi_2 q_2(\phi(\psi+\mu+\delta)+\alpha)}{(\pi+\alpha+\mu)(\psi+\mu+\delta)} & \frac{\xi_2 q_2}{(\psi+\mu+\delta)} & 0 \\ 0 & \lambda & 0 \\ 0 & 0 & \lambda \end{bmatrix} = 0. \tag{96}$$

On solving Equation (96), we have

$$\lambda_1 = \frac{\xi_2 q_2(\phi(\psi+\mu+\delta)+\alpha)}{(\pi+\alpha+\mu)(\psi+\mu+\delta)}, \lambda_2 = 0 \text{ and } \lambda_3 = 0. \tag{97}$$

Thus, the effective reproduction number, R_{HCV}, for the HCV-only submodel is given by

$$R_{HCV} = \frac{\xi_2 q_2(\phi(\psi+\mu+\delta)+\alpha)}{(\pi+\alpha+\mu)(\psi+\mu+\delta)}. \tag{98}$$

The parameters that are crucial in increasing or decreasing the value of R_{HCV} are discussed under sensitivity analysis in Section 4.

Lemma 6. *The stability of the HCV infection-free equilibrium E^0_{HCV}, depends on R_{HCV} being locally asymptotically stable for $R_{HCV} < 1$ and unstable for $R_{HCV} > 1$.*

Proof 9. The Jacobian matrix, $J(E^0_{HCV})$ at the HCV infection-free equilibrium, of the HCV-only submodel (85) is given by

$$J(E^0_{HCV}) = \begin{bmatrix} -\mu & \pi - \xi_2 q_2 \phi & -\xi_2 q_2 & \nu_1 \\ 0 & \xi_2 q_2 \phi - (\pi+\alpha+\mu) & \xi_2 q_2 & 0 \\ 0 & \alpha & -(\psi+\mu+\delta) & 0 \\ 0 & 0 & \psi & -(\mu+\nu_1) \end{bmatrix}. \tag{99}$$

Now, the characteristic polynomial $P(\lambda)$ is given by

$$P(\lambda) = \det\begin{bmatrix} (\lambda+\mu) & \pi - \xi_2 q_2 \phi & -\xi_2 q_2 & \nu_1 \\ 0 & \lambda + (\pi+\alpha+\mu) - \xi_2 q_2 \phi & \xi_2 q_2 & 0 \\ 0 & \alpha & \lambda + (\psi+\mu+\delta) & 0 \\ 0 & 0 & \psi & \lambda + (\mu+\nu_1) \end{bmatrix}. \tag{100}$$

On solving Equation (100), we have

$$P(\lambda) = (\lambda+\mu)(\lambda + (\mu+\nu_1))\left(\lambda^2 + a_1\lambda + a_0\right), \tag{101}$$

where

$$a_1 = (\psi+\mu+\delta) + (\pi+\alpha+\mu) - \xi_2 q_2 \phi > 0 \text{ provided } (\psi+\mu+\delta) + (\pi+\alpha+\mu) > \xi_2 q_2 \phi \tag{102}$$

and

$$\begin{aligned} a_0 &= (\psi+\mu+\delta)((\pi+\alpha+\mu) - \xi_2 q_2 \phi) - \alpha \xi_2 q_2, \\ &= (\psi+\mu+\delta)(\pi+\alpha+\mu)(1 - R_{HCV}) > 0, \quad \text{if } R_{HCV} < 1. \end{aligned} \tag{103}$$

By Routh-Hurwitz criterion, the characteristic polynomial $\lambda^2 + a_1\lambda + a_0$ has negative eigenvalues if $a_1 > 0$ and $a_0 > 0$ which is satisfied when $R_{HCV} < 1$.

4185, 2026, 1, Downloaded from https://onlinelibrary.wiley.com/doi/10.1155/jama/8033235 by Readcube (Labtiva Inc.), Wiley Online Library on [12/11/2026]. See the Terms and Conditions (https://onlinelibrary.wiley.com/terms-and-conditions) on Wiley Online Library for rules of use; OA articles are governed by the applicable Creative Commons License

Therefore, since all the eigenvalues of the characteristic polynomial of Equation (101) are negative for $R_{HCV} < 1$, then the HCV infection-free equilibrium point of system (85) is locally asymptotically stable. □

3.4.1 | Global Stability of HCV Infection-Free Equilibrium for HCV-Only Submodel

The global behaviour of HCV-only submodel (85) is studied by applying the theorem by Castillo-Chavez et al. [44].

Re-writing the HCV-only submodel (85) in the form:

$$\begin{aligned}\frac{dX_{HCV}}{dt} &= F(X_{HCV}, Z_{HCV}),\\ \frac{dZ_{HCV}}{dt} &= G_{HCV}(X_{HCV}, Z_{HCV}),\ G_{HCV}(X_{HCV}, 0) = 0,\end{aligned} \tag{104}$$

where $X_{HCV} = (S)$ and $Z_{HCV} = (I_A, I_C, R_H)$, with $X_{HCV} \in \mathbb{R}_+$ denoting (its components) the number of uninfected humans and $Z_{HCV} \in \mathbb{R}_+^3$ whose elements signify the HCV-infected individuals including those ones under treatment class. Let the HCV infection-free equilibrium of system (104) be denoted by $E^0_{HCV} = (X^0_{HCV}, 0) = (\Lambda/\mu, 0, 0, 0)$.

Now, the following conditions need to be satisfied to guarantee global asymptotic stability.

$$\begin{aligned}&E1\text{: For}\frac{dX_{HCV}}{dt} = F(X_{HCV}, 0), X^0_{HCV}\\ &\quad\text{is globally asymptotically stable.}\\ &E2\text{: } G_{HCV}(X_{HCV}, Z_{HCV}) = AZ_{HCV} - \widehat{G_{HCV}}(X_{HCV}, Z_{HCV}),\\ &\quad\widehat{G_{HCV}}(X_{HCV}, Z_{HCV}) \geq 0, \quad \text{for}\,(X_{HCV}, Z_{HCV}) \in \Omega_{HCV},\end{aligned} \tag{105}$$

where $A = \partial/\partial Z_{HCV} G_{HCV}(X^0_{HCV}, 0)$ is a Metzler matrix and Ω_{HCV} is the invariant region in which the model makes biological sense.

Theorem 4. *The fixed point $E^0_{HCV} = (X_{HCV}, 0)$ is a globally asymptotic stable equilibrium of (104) provided $R_{HCV} < 1$ and that the conditions (E1) and (E2) are satisfied.*

Proof 10. From Lemma 6, E^0_{HCV} is locally asymptotically stable if $R_{HCV} < 1$. □

Regarding the first condition (E1), which pertains to the global asymptotic stability of X^0_{HCV}, we have

$$F(X_{HCV}, Z_{HCV}) = \begin{bmatrix} \Lambda + \pi I_A + \nu_1 R_H - (\lambda_H + \mu)S \\ 0 \end{bmatrix}, \tag{106}$$

and

$$\frac{dX_{HCV}}{dt} = F(X_{HCV}, 0) = \Lambda - \mu S, \tag{107}$$

which is a linear differential equation. On solving Equation (107), we get

$$S(t) = \frac{\Lambda}{\mu} - \frac{\Lambda}{\mu}e^{-\mu t} + S(0)e^{-\mu t}. \tag{108}$$

In the limit as t goes to infinity, $S(t)$ approaches Λ/μ, independent of the starting value of $S(0)$. Consequently, the fact that the solution converges to Ω_{HCV}, implies condition (E1) holds true.

For the second condition, (E2), consider

$$G_{HCV}(X_{HCV}, Z_{HCV}) = \begin{bmatrix} \xi_2 q_2 \dfrac{(\phi I_A + I_C)S}{N_{HCV}} - (\pi + \alpha + \mu)I_A \\ \alpha I_A - (\psi + \mu + \delta) \\ \psi I_C - (\mu + \nu_1)R_H \end{bmatrix}, \tag{109}$$

and

$$A = \begin{bmatrix} \xi_2 q_2 \phi \dfrac{S}{N_{HCV}} - (\pi + \alpha + \mu) & \xi_2 q_2 \dfrac{S}{N_{HCV}} & 0 \\ \alpha & -(\psi + \mu + \delta) & 0 \\ 0 & \psi & -(\mu + \nu_1) \end{bmatrix}. \tag{110}$$

Now, at

$$E^0_{HCV} = \left(\frac{\Lambda}{\mu}, 0, 0, 0\right), \quad \frac{S}{N_{HCV}} \leq 1. \tag{111}$$

Thus,

$$A = \begin{bmatrix} \xi_2 q_2 \phi - (\pi + \alpha + \mu) & \xi_2 q_2 & 0 \\ \alpha & -(\psi + \mu + \delta) & 0 \\ 0 & \psi & -(\mu + \nu_1) \end{bmatrix}, \tag{112}$$

and

$$\begin{aligned}&\widehat{G_{HCV}}(X_{HCV}, Z_{HCV}) = AZ_{HCV} - G_{HCV}(X_{HCV}, Z_{HCV}),\\ &\widehat{G_{HCV}}(X_{HCV}, Z_{HCV}) = \begin{bmatrix} \xi_2 q_2 \phi I_A\left(1 - \dfrac{S}{N_{HCV}}\right) + \xi_2 q_2 I_C\left(1 - \dfrac{S}{N_{HCV}}\right) \\ 0 \\ 0 \end{bmatrix}.\end{aligned} \tag{113}$$

Since $0 < S \leq N_{HCV}$, it is clearly noticeable from Equation (113) that $\widehat{G_{HCV}}(X_{HCV}, Z_{HCV}) \geq 0$. However, matrix A is not a Metzler matrix since not all it off-diagonal elements are non-negative. Hence, E^0_{HCV} may lack global asymptotic stability for $R_{HCV} < 1$. Consequently, a backward bifurcation takes place as established by Feng at el. [49] at $R_{HCV} = 1$. The system can exhibit bistability, where both disease-free and disease-present states co-exist and the initial conditions determine which state the system converges to.

3.5 | HCV-Only Endemic Equilibrium Point

The HCV infection equilibrium point, $E^*_{HCV} = (S^*, I^*_A, I^*_C, R^*_H)$, occurs when HCV infection persists in the population. The derivatives of HCV-only submodel (85) are equated to zero, giving the HCV infection endemic equilibrium point, E^*_{HCV}, as

4185, 2026, 1, Downloaded from https://onlinelibrary.wiley.com/doi/10.1155/jama/8033235 by Readcube (Labtiva Inc.), Wiley Online Library on [12/11/2026]. See the Terms and Conditions (https://onlinelibrary.wiley.com/terms-and-conditions) on Wiley Online Library for rules of use; OA articles are governed by the applicable Creative Commons License

$$\left(\frac{(\pi+\alpha+\mu)(\psi+\mu+\delta)N^*_{HCV}}{\xi_2 q_2(\phi(\psi+\mu+\delta)+\alpha)}, \frac{(\psi+\mu+\delta)(\Lambda-\mu N^*_{HCV})}{\alpha\delta}, \frac{(\Lambda-\mu N^*_{HCV})}{\delta}, \frac{\psi(\Lambda-\mu N^*_{HCV})}{\delta(\mu+\nu_1)}\right). \tag{114}$$

Lemma 7. *The HCV-only submodel (85) has a unique endemic equilibrium point if $R_{HCV} > 1$.*

Proof 11. If the disease stays in the population, then $dI_A/dt > 0$ and $dI_C/dt > 0$, that is

$$\xi_2 q_2(\phi I_A + I_C)\frac{S}{N_{HCV}} - (\pi+\alpha+\mu)I_A > 0, \tag{115}$$

$$\alpha I_A - (\psi+\mu+\delta)I_C > 0. \tag{116}$$

□

Re-arranging inequality (115), we have

$$I_A < \frac{\xi_2 q_2(\phi I_A + I_C)}{(\pi+\alpha+\mu)}\frac{S}{N_{HCV}}. \tag{117}$$

Using the fact that $S/N_{HCV} \leq 1$, inequality (117) reduces to

$$I_A < \frac{\xi_2 q_2(\phi I_A + I_C)}{(\pi+\alpha+\mu)}. \tag{118}$$

From inequality (116), we have

$$I_C < \frac{\alpha I_A}{(\psi+\mu+\delta)}. \tag{119}$$

Substituting I_C into inequality (118) and simplifying, we get

$$1 < \frac{\xi_2 q_2(\phi(\pi+\alpha+\mu)+\alpha)}{(\pi+\alpha+\mu)(\psi+\mu+\delta)}. \tag{120}$$

Thus, $R_{HCV} > 1$.

Hence, a unique endemic equilibrium point E^*_{HCV} exists when $R_{HCV} > 1$.

Lemma 8. *The HCV infection endemic equilibrium point $E^*_{HCV} = (S^*, I^*_A, I^*_C, R^*_H)$ is locally asymptotically stable for the effective reproduction number, $R_{HCV} > 1$, and unstable otherwise.*

Proof 12. To study the local stability of the HCV endemic equilibrium point, we use the method of Routh-Hurwitz criterion. At the HCV endemic equilibrium point, E^*_{HCV}, the Jacobian matrix is

$$J(E^*_{HCV}) = \begin{bmatrix} -(f^*+\mu) & \pi - \frac{\xi_2 q_2 \phi}{R_{HCV}} & \frac{-\xi_2 q_2}{R_{HCV}} & \nu_1 \\ f^* & \frac{\xi_2 q_2 \phi}{R_{HCV}} - (\pi+\alpha+\mu) & \frac{\xi_2 q_2}{R_{HCV}} & 0 \\ 0 & \alpha & -(\psi+\mu+\delta) & 0 \\ 0 & 0 & \psi & -(\mu+\nu_1) \end{bmatrix}, \tag{121}$$

where

$$f^* = \frac{\xi_2 q_2(\Lambda-\mu N_{HCV})(\phi(\psi+\mu+\delta)+\alpha)}{\alpha\delta N_{HCV}}, \tag{122}$$

is the force of HCV infection evaluated at E^*_{HCV}. The characteristic polynomial $P(\lambda)$ of $J(E^*_{HCV})$ is given as

$$P(\lambda) = \lambda^4 + a_1\lambda^3 + a_2\lambda^2 + a_3\lambda + a_4, \tag{123}$$

where I is a 4×4 identity matrix and

$$\begin{aligned}
a_1 &= (\pi+\alpha+\mu) + (\psi+\mu+\delta) + (\mu+\nu_1) + f^* + \mu \\
&\quad - \frac{\xi_2 q_2 \phi}{R_{HCV}}, \\
a_2 &= 3(\pi+\alpha+\mu)(\psi+\mu+\delta) + (\pi+\alpha+\mu)((\pi+\alpha+\mu)+ \\
&\quad f^*+\mu) - \left(\pi f^* + \frac{\xi_2 q_2 \phi}{R_{HCV}}((\pi+\alpha+\mu)+2(\psi+\mu+\delta)+\mu)\right), \\
a_3 &= (\psi+\mu+\delta)(\mu+\nu_1)((\pi+\alpha+\mu)+(f^*+\mu)) \\
&\quad + (\pi+\alpha+\mu)(f^*+\mu) - (\pi f^*((\psi+\mu+\delta)+(\mu+\nu_1)) \\
&\quad + \frac{\xi_2 q_2}{R_{HCV}}(\phi(\psi+\mu+\delta)(\mu+\nu_1) + \phi\mu((\psi+\mu+\delta) \\
&\quad + (\mu+\nu_1)) + 2\alpha f^* + \alpha(\mu+(\mu+\nu_1))), \\
a_4 &= (\pi+\alpha+\mu)(\psi+\mu+\delta)(\mu+\nu_1)(f^*+\mu) \\
&\quad - ((\psi+\mu+\delta)(\mu+\nu_1)\pi f^* + \alpha\nu_1\psi f^* \\
&\quad + \frac{\xi_2 q_2(\mu+\nu_1)}{R_{HCV}}(\phi(\psi+\mu+\delta)\mu + 2\alpha f^* + \alpha\mu)).
\end{aligned} \tag{124}$$

□

The local stability of the HCV endemic equilibrium is determined by the Routh-Hurwitz criterion which provides the necessary and sufficient conditions. The criterion requires that the Hurwitz determinants, H_i with $i = 1, 2, 3, 4$ are all non-negative. According to the Routh-Hurwitz, for a fourth-degree polynomial, these determinants are given by

$$\begin{aligned}
H_1 &= a_1 > 1, \\
H_2 &= a_1 a_2 - a_3 > 0, \\
H_3 &= a_3(a_1 a_2 - a_3) - a_1^2 a_4 > 0, \\
H_4 &= a_4 > 0.
\end{aligned} \tag{125}$$

When determinants in (125) are satisfied, thus a conclusion can be made that the endemic equilibrium is locally asymptotically stable.

3.5.1 | Global Stability of HCV Endemic Equilibrium for HCV-Only Sub Model

Here, we investigate the global stability of HCV endemic equilibrium point E^*_{HCV}.

Lemma 9. *The HCV infection endemic equilibrium point, E^*_{HCV} for HCV-only submodel is globally asymptotically stable if $R_{HCV} > 1$ and unstable otherwise.*

4185, 2026, 1, Downloaded from https://onlinelibrary.wiley.com/doi/10.1155/jama/8033235 by Readcube (Labtiva Inc.), Wiley Online Library on [12/11/2026]. See the Terms and Conditions (https://onlinelibrary.wiley.com/terms-and-conditions) on Wiley Online Library for rules of use; OA articles are governed by the applicable Creative Commons License

Proof 13. To establish the global asymptotic stability of the HCV endemic equilibrium, we employ the Lyapunov function method. □

We define a Lyapunov function, $= L(S, I_A, I_C, R_H)$, as

$$\begin{aligned} L = {} & U_1\left(S - S^* - S^* In\left(\frac{S}{S^*}\right)\right) + U_2\left(I_A - I_A^* - I_A^* In\left(\frac{I_A}{I_A^*}\right)\right) \\ & + U_3\left(I_C - I_C^* - I_C^* In\left(\frac{I_C}{I_C^*}\right)\right) \\ & + U_4\left(R_H - R_H^* - R_H^* In\left(\frac{R_H}{R_H^*}\right)\right), \end{aligned} \tag{126}$$

where $U_1, U_2, \ldots, U_4$ are positive constants.

Evaluating the derivative of L with respect to time, t along with the equations of system (84), we have

$$\begin{aligned} \frac{dL}{dt} &= U_1\left(1 - \frac{S^*}{S}\right)\frac{dS}{dt} + U_2\left(1 - \frac{I_A^*}{I_A}\right)\frac{dI_A}{dt} \\ &\quad + U_3\left(1 - \frac{I_C^*}{I_C}\right)\frac{dI_C}{dt} + U_4\left(1 - \frac{R_H^*}{R_H}\right)\frac{dR_H}{dt} \\ &= U_1\left(1 - \frac{S^*}{S}\right)(\Lambda + \pi I_A + \nu_1 R_H - \lambda_H S - \mu S) \\ &\quad + U_2\left(1 - \frac{I_A^*}{I_A}\right)(\lambda_H S - (\pi + \alpha + \mu)I_A \\ &\quad + U_3\left(1 - \frac{I_C^*}{I_C}\right)(\alpha I_A - (\psi + \mu + \delta)I_C \\ &\quad + U_4\left(1 - \frac{R_H^*}{R_H}\right)(\psi I_C - (\mu + \nu_1))R_H. \end{aligned} \tag{127}$$

At equilibrium point where HCV infection is endemic, we have:

$$\begin{aligned} \Lambda &= \xi_2 q_2\left(\frac{\phi I_A^* + I_C^*}{N_{HCV}^*}\right)S^* + \mu S^* - \pi I_A^* - \nu_1 R_H^*, \\ (\pi + \alpha + \mu) &= \xi_2 q_2\left(\frac{\phi I_A^* + I_C^*}{N_{HCV}^*}\right)S^*, \\ (\psi + \mu + \delta) &= \frac{\alpha I_A^*}{I_C^*}, \\ (\mu + \nu_1) &= \frac{\psi I_C^*}{R_H^*}. \end{aligned} \tag{128}$$

Substituting Equation (128) into (127), we have

$$\begin{aligned} \frac{dL}{dt} = {} & U_1\left(1 - \frac{S^*}{S}\right)\left(\xi_2 q_2\left(\frac{\phi I_A^* + I_C^*}{N_{HCV}^*}\right)S^* + \mu S^* - \pi I_A^*\right. \\ & \left. - \nu_1 R_H^* + \pi I_A + \nu_1 R_H - \lambda_H S - \mu S\right) \\ & + U_2\left(1 - \frac{I_A^*}{I_A}\right)\left(\lambda_H S - \xi_2 q_2\left(\frac{\phi I_A^* + I_C^*}{N_{HCV}^*}\right)S^* I_A\right) \\ & + U_3\left(1 - \frac{I_C^*}{I_C}\right)\left(\alpha I_A - \frac{\alpha I_A^*}{I_C^*} I_C\right) \\ & + U_4\left(1 - \frac{R_H^*}{R_H}\right)\left(\psi I_C - \frac{\psi I_C^*}{R_H^*} R_H\right). \end{aligned} \tag{129}$$

Now, expanding and collecting positive terms together and negative terms together, we have:

$$\frac{dL}{dt} = A - B, \tag{130}$$

where

$$\begin{aligned} A = {} & U_1\xi_2 q_2\left(\frac{\phi I_A^* + I_C^*}{N_{HCV}^*}\right)S^* + U_1\mu S^* + U_1\pi I_A + U_1\nu_1 R_H \\ & + U_1\pi I_A^*\frac{S^*}{S} U_1\nu_1 R_H^*\frac{S^*}{S} + U_1\xi_2 q_2\left(\frac{\phi I_A + I_C}{N_{HCV}}\right)S + U_1\mu S^* \\ & + U_2\xi_2 q_2\left(\frac{\phi I_A + I_C}{N_{HCV}}\right)S + U_2\xi_2 q_2\left(\frac{\phi I_A^* + I_C^*}{N_{HCV}^*}\right)S^* + U_3\alpha I_A \\ & + U_4\psi I_C + U_4\psi I_C^*, \end{aligned} \tag{131}$$

and

$$\begin{aligned} B = {} & U_1\pi I_A^* + U_1\nu_1 R_H^* + U_1\xi_2 q_2\left(\frac{\phi I_A + I_C}{N_{HCV}}\right)S + U_1\mu S \\ & + U_1\xi_2 q_2\left(\frac{\phi I_A^* + I_C^*}{N_{HCV}^*}\right)S^*\frac{S^*}{S} + U_1\mu S^*\frac{S^*}{S} + U_1\pi I_A\frac{S^*}{S} \\ & + U_1\nu_1 R_H\frac{S^*}{S} + U_2\xi_2 q_2\left(\frac{\phi I_A^* + I_C^*}{N_{HCV}^*}\right)S^*\frac{I_A}{I_A^*} \\ & + U_2\xi_2 q_2\left(\frac{\phi I_A + I_C}{N_{HCV}}\right)S\frac{I_A^*}{I_A} + U_3\alpha_A^*\frac{I_C}{I_A^*} + U_3\alpha I_A\frac{I_C^*}{I_C} \\ & + U_4\psi I_C\frac{R_H}{R_H^*} + U_4\psi I_C\frac{R_H^*}{R_H}. \end{aligned} \tag{132}$$

Thus, we can guarantee that $dL/dt \leq 0$ when $A < B$ and $dL/dt = 0$ when $S = S^*, I_A = I_A^*, I_C = I_C^*$ and $R_H = R_H^*$. Thus, the largest compact set that remains unchanged under the system's evolution in $(S, I_A^*, I_C^*, R^*H) \in \Omega_{HCV}$ such that $dL/dt = 0$ is the single point E_{HCV}^*, where E_{HCV}^* is the HCV endemic equilibrium for HCV-only submodel system. This result, combined with LaSalle's invariant principle [47], it establishes that E_{HCV}^* is globally asymptotically stable in Ω_H when $A < B$.

3.6 | TB–HCV Coinfection Model Analysis

In this subsection, the TB–HCV disease-free equilibrium, E^0, and the effective reproduction number, R_{TH}, for the TB–HCV coinfection model (4) are established.

At the equilibrium point where both TB and HCV are absent, $S^0 = \Lambda/\mu$, $I_L^0 = I_T^0, H^0 = R_T^0 = I_A^0 = I_C^0 = R_H^0 = I_{AL}^0 = I_{CL}^0 = I_{AT}^0 = I_{CT}^0 = R^0 = 0$.

Therefore, the disease-free equilibrium point is given by

$$E^0 = \left(\frac{\Lambda}{\mu}, 0, 0, 0, 0, 0, 0, 0, 0, 0, 0, 0, 0\right). \tag{133}$$

Lemma 10. *The effective reproduction number for TB–HCV coinfection model,* $R_{TH} = \max\{R_{TB}, R_{HCV}\}$.

Proof 14. The next generation method is used to calculate R_0. Now, using the method in [42, 48, 50, 51] on TB–HCV coinfection

4185, 2026, 1, Downloaded from https://onlinelibrary.wiley.com/doi/10.1155/jama/8033235 by Readcube (Labtiva Inc.), Wiley Online Library on [12/11/2026]. See the Terms and Conditions (https://onlinelibrary.wiley.com/terms-and-conditions) on Wiley Online Library for rules of use; OA articles are governed by the applicable Creative Commons License

model system (4), the matrices representing the rate of new infection emergence F_i, in compartment i, and the rate of exchange between compartment i and other components through various processes, V_i, are obtained as follows:

$$F = \begin{bmatrix} 0 & \xi_1 q_1 & \xi_1 q_1 \epsilon & 0 & 0 & 0 & 0 & 0 & 0 & \xi_1 q_1 & \xi_1 q_1 a_2 & 0 \\ 0 & 0 & 0 & 0 & 0 & 0 & 0 & 0 & 0 & 0 & 0 & 0 \\ 0 & 0 & 0 & 0 & 0 & 0 & 0 & 0 & 0 & 0 & 0 & 0 \\ 0 & 0 & 0 & 0 & 0 & 0 & 0 & 0 & 0 & 0 & 0 & 0 \\ 0 & 0 & 0 & 0 & \xi_2 q_2 \phi & \xi_2 q_2 & 0 & \xi_2 q_2 b_1 & \xi_2 q_2 b_2 & \xi_2 q_2 b_3 & \xi_2 q_2 b_4 & 0 \\ 0 & 0 & 0 & 0 & 0 & 0 & 0 & 0 & 0 & 0 & 0 & 0 \\ 0 & 0 & 0 & 0 & 0 & 0 & 0 & 0 & 0 & 0 & 0 & 0 \\ 0 & 0 & 0 & 0 & 0 & 0 & 0 & 0 & 0 & 0 & 0 & 0 \\ 0 & 0 & 0 & 0 & 0 & 0 & 0 & 0 & 0 & 0 & 0 & 0 \\ 0 & 0 & 0 & 0 & 0 & 0 & 0 & 0 & 0 & 0 & 0 & 0 \\ 0 & 0 & 0 & 0 & 0 & 0 & 0 & 0 & 0 & 0 & 0 & 0 \\ 0 & 0 & 0 & 0 & 0 & 0 & 0 & 0 & 0 & 0 & 0 & 0 \end{bmatrix}. \tag{134}$$

$$F_i = \begin{bmatrix} \lambda_T S \\ 0 \\ 0 \\ 0 \\ \lambda_H S \\ 0 \\ 0 \\ \lambda_T I_A + \lambda_H I_L \\ \lambda_T I_C \\ \lambda_H I_T \\ 0 \\ 0 \end{bmatrix}, \tag{135}$$

and

$$V_i = \begin{bmatrix} -p_1\pi I_{AL} + (\theta + \eta + \mu + \lambda_H) I_L \\ -\theta I_L + (\omega_1 + \rho + \mu + \sigma_1 + \lambda_H) I_T \\ -\rho I_T + (\omega_2 + \mu + \sigma_2) H \\ -\omega_2 H - \omega_1 I_T + (\nu_2 + \mu) R_T \\ -p_2\eta I_{AL} + (\pi + \alpha + \mu + \lambda_T) I_A \\ -\alpha I_A + (\psi + \mu + \delta + \lambda_H) I_C \\ -\psi I_C + (\nu_1 + \mu) R_H \\ (\tau_1 + \mu + \beta_1 + \gamma + p_1\pi + p_2\eta) I_{AL} \\ -\beta_1 I_{AL} + (r_1 + \tau_2 + \mu + \delta) I_{CL} \\ -\tau_1 I_{AL} + (r_2 + \beta_2 + \mu + d_1) I_{AT} \\ -\tau_2 I_{CL} - \beta_2 I_{AT} + (r_3 + \mu + d_2) I_{CT} \\ -r_1 I_{CL} - r_2 I_{AT} - r_3 I_{CT} + (\nu_3 + \mu) R \end{bmatrix}. \tag{136}$$

□

The Jacobian matrix, F, of the new infection emergence at disease-free equilibrium point, E^0, is given in Equation (134).

The rate of exchange between compartment i and other compartments through various processes at the disease-free equilibrium point E^0 are represented by the Jacobian matrix V, which is given by

$$V = \begin{bmatrix} h_1 & 0 & 0 & 0 & 0 & 0 & 0 & -p_1\pi & 0 & 0 & 0 & 0 \\ -\theta & h_2 & 0 & 0 & 0 & 0 & 0 & 0 & 0 & 0 & 0 & 0 \\ 0 & -\rho & h_3 & 0 & 0 & 0 & 0 & 0 & 0 & 0 & 0 & 0 \\ 0 & \omega_1 & -\omega_2 & h_4 & 0 & 0 & 0 & 0 & 0 & 0 & 0 & 0 \\ 0 & 0 & 0 & 0 & h_5 & 0 & 0 & -p_2\eta & 0 & 0 & 0 & 0 \\ 0 & 0 & 0 & 0 & -\alpha & h_6 & 0 & 0 & 0 & 0 & 0 & 0 \\ 0 & 0 & 0 & 0 & 0 & \psi & h_7 & 0 & 0 & 0 & 0 & 0 \\ 0 & 0 & 0 & 0 & 0 & 0 & 0 & h_8 & 0 & 0 & 0 & 0 \\ 0 & 0 & 0 & 0 & 0 & 0 & 0 & -\beta_1 & h_9 & 0 & 0 & 0 \\ 0 & 0 & 0 & 0 & 0 & 0 & 0 & -\tau_1 & 0 & h_{10} & 0 & 0 \\ 0 & 0 & 0 & 0 & 0 & 0 & 0 & 0 & -\tau_2 & -\beta & h_{11} & 0 \\ 0 & 0 & 0 & 0 & 0 & 0 & 0 & 0 & -r_1 & -r_2 & -r_3 & h_{12} \end{bmatrix},$$

where

$$\begin{aligned} &h_1 = (\theta + \eta + \mu), h_2 = (\omega_1 + \rho + \mu + \sigma_1), \\ &h_3 = (\omega_2 + \mu + \sigma_2), h_4 = (\nu_2 + \mu), h_5 = (\pi + \alpha + \mu), \\ &h_6 = (\psi + \mu + \delta), h_7 = (\nu_1 + \mu), \\ &h_8 = (\tau_1 + \mu + \beta_1 + \gamma + p_1\pi + p_2\eta), \\ &h_9 = (r_1 + \tau_2 + \mu + \delta), h_{10} = (r_2 + \beta_2 + \mu + d_1), \\ &h_{11} = (r_3 + \mu + d_2), h_{12} = (\nu_3 + \mu). \end{aligned} \tag{137}$$

4185, 2026, 1, Downloaded from https://onlinelibrary.wiley.com/doi/10.1155/jama/8033235 by Readcube (Labtiva Inc.), Wiley Online Library on [12/11/2026]. See the Terms and Conditions (https://onlinelibrary.wiley.com/terms-and-conditions) on Wiley Online Library for rules of use; OA articles are governed by the applicable Creative Commons License

However, the effective reproduction number, R_{TH}, for the TB–HCV coinfection model is the greatest of eigenvalues $\lambda_1, \lambda_2, \lambda_3, \lambda_4, \lambda_5, \lambda_6, \lambda_7, \lambda_8, \lambda_9, \lambda_{10}, \lambda_{11}$ and λ_{12} of the next generation matrix, FV^{-1}. That is,

$$R_{TH} = \max\left\{\frac{\xi_1 q_1 \theta}{(\eta+\mu+\theta)(\omega_1+\rho+\mu)}\left(1+\frac{\epsilon\rho}{(\omega_2+\mu+\sigma_2)}\right),\right.$$
$$\left.\frac{\xi_2 q_2(\phi(\psi+\mu+\delta)+\alpha)}{(\pi+\alpha+\mu)(\psi+\mu+\delta)}, 0, 0, 0, 0, 0, 0, 0, 0, 0, 0\right\}. \tag{138}$$

Therefore,

$$R_{TH} = \max\{R_{TB}, R_{HCV}\}, \tag{139}$$

where R_{TB} and R_{HCV} are the effective reproduction numbers of TB and HCV-only submodels, respectively. This means that the spread of TB–HCV coinfection will be largely influenced by the disease with higher transmission potential.

The following Theorem 5 is a consequence of Theorem 2 of Van den Driessche and Watmough [42].

Theorem 5. *The disease-free equilibrium point, E^0, in the TB–HCV coinfection model (4) is stable locally if $R_{TH} < 1$ and loses stability when $R_{TH} > 1$.*

3.6.1 | Global Stability of Disease-Free Equilibrium Point for TB–HCV Coinfection Model

In order to investigate the global stability of the disease-free equilibrium point, E^0, for the TB–HCV coinfection model System (4), we apply the same approach used by Castillo-Chavez et al. [44].

Rewriting the TB–HCV coinfection model (4) in the following form:

$$\frac{dX}{dt} = F(X, Z)$$
$$\frac{dZ}{dt} = G(X, Z), G(X, 0) = 0, \tag{140}$$

where $X = (S)$ and $Z = (I_L, I_T, H, R_T, I_A, I_C, R_H, I_{AL}, I_{CL}, I_{AT}, I_{CT}, R)$, with $X \in R_+$ denoting the number of uninfected humans and $Z \in R_+^{12}$ whose elements represent individuals infected with TB, HCV or both TB and HCV including those under treatment of TB or HCV.

Let $E^0 = (X^0, 0) = (\Lambda/\mu, 0)$ be the disease-free equilibrium of system (140). To ensure global asymptotic stability, we need to ascertain that conditions (S_1) and (S_2) are satisfied.

$$(S_1)\text{: For}\frac{dX}{dt} = F(X, 0), X^0 \text{is globally asymptotically stable},$$
$$(S_2)\text{: } G(X, Z) = NZ - \widehat{G}(X, Z) \geq 0, \quad \text{for}(X, Z) \in \Omega, \tag{141}$$

where $N = D_Z G(X^0, 0)$ is a Metzler matrix and Ω is the domain where the model is biologically applicable. Therefore, provided system (140) satisfies conditions (S_1) and (S_2), Theorem 6 holds true.

Theorem 6. *The equilibrium point $E^0 = (X, 0)$ is an attractor for all initial conditions of system (140) provided $R_{TH} < 1$ and that the conditions (S1) and (S2) are fulfilled.*

Proof 15. From Theorem 5, E^0 is locally asymptotically stable if $R_{TH} < 1$. □

Considering the first condition $(S1)$, that is, the global attractivity of X^0, we have

$$F(X, Z) = \begin{bmatrix} \Lambda + \nu_1 R_H + \nu_2 R_T + \nu_3 R + \pi I_A + \eta I_L + \gamma I_{AL} - (\lambda_T + \lambda_H + \mu)S \\ 0 \end{bmatrix}, \tag{142}$$

and

$$\frac{dX}{dt} = F(X, 0) = \Lambda - \mu S, \tag{143}$$

which takes the form of a linear differential equation. Solving Equation (143), gives

$$S(t) = \frac{\Lambda}{\mu} - \frac{\Lambda}{\mu}e^{-\mu t} + S(0)e^{-\mu t}. \tag{144}$$

As t, increases without bound $S(t) \longrightarrow \Lambda/\mu$ irrespective of the value of $S(0)$. Thus, a convergence in Ω, signifying that condition $(S1)$ holds true.

For the second condition, $(S2)$, we consider

$$G(X, Z) = \begin{bmatrix} \lambda_T S + p_1\pi I_{AL} - (\theta+\eta+\mu+\lambda_H)I_L \\ \theta I_L - (\omega_1+\rho+\mu+\sigma_1+\lambda_H)I_T \\ \rho I_T - (\omega_2+\mu+\sigma_2)H \\ \omega_2 H + \omega_1 I_T - (\nu_2+\mu)R_T \\ \lambda_H S + p_2\eta I_{AL} - (\pi+\alpha+\mu+\lambda_T)I_A \\ \alpha I_A - (\psi+\mu+\delta+\lambda_T)I_C \\ \psi I_C - (\nu_1+\mu)R_H \\ \lambda_T I_A + \lambda_H I_L - (\tau_1+\mu+\beta_1+\gamma+p_1\pi+p_2\eta)I_{AL} \\ \beta_1 I_{AL} + \lambda_T I_C - (r_1+\tau_2+\mu+\delta)I_{CL} \\ \tau_1 I_{AL} + \lambda_H I_T - (r_2+\beta_2+\mu+d_1)I_{AT} \\ \tau_2 I_{CL} + \beta_2 I_{AT} - (r_3+\mu+d_2)I_{CT} \\ r_1 I_{CL} + r_2 I_{AT} + r_3 I_{CT} - (\nu_3+\mu)R \end{bmatrix}, \tag{145}$$

and

4185, 2026, 1, Downloaded from https://onlinelibrary.wiley.com/doi/10.1155/jama/8033235 by Readcube (Labtiva Inc.), Wiley Online Library on [12/11/2026]. See the Terms and Conditions (https://onlinelibrary.wiley.com/terms-and-conditions) on Wiley Online Library for rules of use; OA articles are governed by the applicable Creative Commons License

$$K=\begin{bmatrix} -j_1 & \xi_1 q_1 & \xi_1 q_1 \epsilon & 0 & 0 & 0 & 0 & p_1\pi & 0 & \xi_1 q_1 a_1 & \xi_1 q_1 a_2 & 0 \\ \theta & -j_2 & 0 & 0 & 0 & 0 & 0 & 0 & 0 & 0 & 0 & 0 \\ 0 & \rho & -j_3 & 0 & 0 & 0 & 0 & 0 & 0 & 0 & 0 & 0 \\ 0 & \omega_1 & \omega_2 & -j_4 & 0 & 0 & 0 & 0 & 0 & 0 & 0 & 0 \\ 0 & 0 & 0 & 0 & -j_5 & \xi_2 q_2 & 0 & \xi_2 q_2 b_1 + p_2\eta & \xi_2 q_2 b_2 & \xi_2 q_2 b_3 & \xi_2 q_2 b_4 & 0 \\ 0 & 0 & 0 & 0 & \alpha & -j_6 & 0 & 0 & 0 & 0 & 0 & 0 \\ 0 & 0 & 0 & 0 & 0 & \psi & -j_7 & 0 & 0 & 0 & 0 & 0 \\ 0 & 0 & 0 & 0 & 0 & 0 & 0 & -j_8 & 0 & 0 & 0 & 0 \\ 0 & 0 & 0 & 0 & 0 & 0 & 0 & \beta_1 & -j_9 & 0 & 0 & 0 \\ 0 & 0 & 0 & 0 & 0 & 0 & 0 & \tau_1 & 0 & -j_{10} & 0 & 0 \\ 0 & 0 & 0 & 0 & 0 & 0 & 0 & 0 & \tau_2 & \beta_2 & -j_{11} & 0 \\ 0 & 0 & 0 & 0 & 0 & 0 & 0 & 0 & r_1 & r_2 & r_3 & -j_{12} \end{bmatrix}, \tag{146}$$

where

$$\begin{aligned} &j_1=(\theta+\eta+\mu), j_2=(\omega_1+\rho+\mu+\sigma_1),\\ &j_3=(\omega_2+\mu+\sigma_2), j_4=(\nu_2+\mu),\\ &j_5=\xi_2 q_2\phi-(\pi+\alpha+\mu), j_6=(\psi+\mu+\delta),\\ &j_7=(\nu_1+\mu), j_8=(\tau_1+\mu+\beta_1+\gamma+p_1\pi+p_2\eta),\\ &j_9=(r_1+\tau_2+\mu+\delta),\\ &j_{10}=(r_2+\beta_2+\mu+d_1), j_{11}=(r_3+\mu+d_2), j_{12}=(\nu_3+\mu). \end{aligned} \tag{147}$$

Then,

$$\begin{aligned} \widehat{G}(X,Z)&=\begin{bmatrix} \widehat{G}_1(X,Z)\\ \widehat{G}_2(X,Z)\\ \widehat{G}_3(X,Z)\\ \widehat{G}_4(X,Z)\\ \widehat{G}_5(X,Z)\\ \widehat{G}_6(X,Z)\\ \widehat{G}_7(X,Z)\\ \widehat{G}_8(X,Z)\\ \widehat{G}_9(X,Z)\\ \widehat{G}_{10}(X,Z)\\ \widehat{G}_{11}(X,Z)\\ \widehat{G}_{12}(X,Z) \end{bmatrix}\\ &=KZ-G(X,Z), \end{aligned}$$

$$=\begin{bmatrix} \lambda_H I_L+\xi_1 q_1\left(1-\frac{S}{N}\right)(I_T+\epsilon H+a_1 I_{AT}+a_2 I_{CT})\\ \theta I_L+\lambda_H I_T\\ 0\\ 0\\ \lambda_T I_A+\xi_2 q_2(\phi I_A+I_C+b_1 I_A+b_2 I_C+b_3 I_{AT}+b_4 I_{CT})\left(1-\frac{S}{N}\right)\\ \lambda_T I_C\\ 0\\ -(\lambda_T I_A+\lambda_H I_L)\\ -\lambda_T I_C\\ -\lambda_H I_T\\ 0\\ 0 \end{bmatrix}. \tag{148}$$

Since $\widehat{G}_8(X,Z)<0\,\widehat{G}_9(X,Z)<0\,\text{and}\,\widehat{G}_{10}(X,Z)<0$, which implies that condition (S_2) does not hold. Thus, $E_0=(X^0,0)$ may not be stable in the long run for $R_{TH}<1$. This analysis predicts a backward bifurcation at $R_{TH}=1$ as demonstrated by Feng et al. [49]. In a biological context, backward bifurcation indicates that a stable state with ongoing transmission and state with no infection can simultaneously exist when the effective reproduction number is less than unity. It further illustrates that an occurrence due to the disease may persist even if the effective reproduction number is reduced to one.

4 | Existence and Stability of TB–HCV Coinfection Endemic Equilibrium

The analytical determination of the steady state where both TB and HCV are endemic is strenuous. Thus, its existence and stability is verified through numerical simulations as demonstrated in study [39].

4185, 2026, 1, Downloaded from https://onlinelibrary.wiley.com/doi/10.1155/jama/8033235 by Readcube (Labtiva Inc.), Wiley Online Library on [12/11/2026]. See the Terms and Conditions (https://onlinelibrary.wiley.com/terms-and-conditions) on Wiley Online Library for rules of use; OA articles are governed by the applicable Creative Commons License

The initial states of the variables, $S, I_L, I_T, H, R_T I_A, I_C, R_H, I_{AL}, I_{CL}, I_{AT}, I_{CT}$ and R, are adjusted to determine if they converge to the same positive equilibrium values over time despite different initial variable values. The values of the parameters used in the numerical study are presented in Table 2.

Now, in Figure 2, the starting values of the specified variable are adjusted while holding the starting values of other variables of the TB–HCV coinfection model constant so as to establish whether they converge to the same positive equilibrium values over time despite different initial variable values. Curves in Figure 2 eventually converge to the same positive equilibrium values over time despite different initial variable values.

In Figure 3, we further demonstrate the existence and stability of the endemic state of the TB–HCV coinfection model. The values of some singled-out parameters say, the rate of human-to-human contact between the TB-infected individuals and susceptible population, ξ_1 and the rate of human-to-human contact between the HCV-infected individuals and susceptible population, ξ_2 are varied for some singled-out variables, say, TB infectious individuals assumed not on medication, I_T, acute HCV infected individuals, I_A, chronic HCV-infected individuals, I_C and dually infected individuals with chronic HCV infections in the TB infectious stage, I_{CT}. This is done to ascertain whether these variables would in the due course level off to nonzero values regardless of the varying values of ξ_1 and ξ_2. Figure 3 reveals that despite the varying values of ξ_1 and ξ_2, in the long term, I_T, I_A, I_C and I_{CT} attain a nonzero steady state, hence verifying the presence of a globally stable endemic equilibrium for the TB–HCV coinfection model.

TABLE 2 | The TB–HCV coinfection model parameter values.

Parameter	Value/yr^{-1}	Source
μ	0.02	[16]
σ_1	0.0575	[19]
σ_2	0.00205	[20]
δ	0.82	[23]
d_1	0.6	Assumed
d_2	0.8	Assumed
θ	0.25	[32]
ρ	0.0415	[20]
ω_1	0.7311	[19]
ω_2	0.8733	[20]
α	2	[16]
ψ	0.30	[16]
ϵ	0.35	Assumed
τ_1	0.00013	Assumed
τ_2	0.00015	Assumed
β_1	0.00014	Assumed
β_2	0.00016	Assumed
r_1	0.5	Assumed
r_2	0.6	Assumed
r_3	0.4	Assumed
ν_1	0.025	[16]
ν_2	0.03	[32]
ν_3	0.05	Assumed
η	0.4405	[32]
π	0.27	[16]
ϕ	0.20	Assumed
γ	0.05	Assumed
ξ_1, ξ_2	4, 2 people	[16, 32]
q_1, q_2	0.08, 0.07	[16, 32]
a	1.002	Assumed
b_1, b_2, b_3 and b_4	1.003, 1.002, 1.005, 1.001	Assumed
p_1, p_2	0.4, 0.2	Assumed

4.1 | Sensitivity Analysis

The sensitivity analysis is performed to assess the model's ability to withstand parameter fluctuations. This analysis can reveal which parameter has the greatest influence on R_{TH} [52, 53]. Additionally, it facilitates the assessment of the relative impact of parameter changes on the state variable [52]. The normalised forward sensitivity index shall be used to assess the sensitivity of each parameter of the model [39, 54].

Definition 1. Let the variable W be a differentiable function of the parameter, p, then the normalised forward sensitivity index of a variable W with respect to a parameter p is defined as

$$i_p^W = \frac{\partial W}{\partial p} \times \frac{p}{W}. \tag{149}$$

4.1.1 | Computation of Sensitivity Indices of the Basic Reproduction Numbers With Respect to the Parameters of the Model

Now, we proceed to perform the sensitivity analysis of the effective reproduction number of the TB–HCV coinfection model, R_{TH}, to each of the parameter by computing the sensitivity indices of R_{TH} with respect to the parameters of the model using the normalised forward sensitivity index method [52].

Since $R_{TH} = \max\{R_{TB}, R_{HCV}\}$, sensitivity analysis of R_{TH} with respect to each of the parameters is carried out separately for R_{TB} and R_{HCV}. The sensitivity indices of R_{TB} and R_{HCV} have been calculated using formulaes (149) and (150), respectively:

$$i_p^{R_{TB}} = \frac{\partial R_{TB}}{\partial p} \times \frac{p}{R_{TB}}, \tag{150}$$

and

$$i_p^{R_{HCV}} = \frac{\partial R_{HCV}}{\partial p} \times \frac{p}{R_{HCV}}. \tag{151}$$

The parameter values used with their respective sources and others assumed are presented in Table 2.

The sensitivity indices of R_{TB} and R_{HCV} are summarised in Table 3, in which parameters are in order of sensitivity.

4.2 | Analysis of Sensitivity Results

The sensitivity indices presented in Table 3 are explained in such a way that, when a parameter with a positive sensitivity index

4185, 2026, 1, Downloaded from https://onlinelibrary.wiley.com/doi/10.1155/jama/8033235 by Readcube (Labtiva Inc.), Wiley Online Library on [12/11/2026]. See the Terms and Conditions (https://onlinelibrary.wiley.com/terms-and-conditions) on Wiley Online Library for rules of use; OA articles are governed by the applicable Creative Commons License

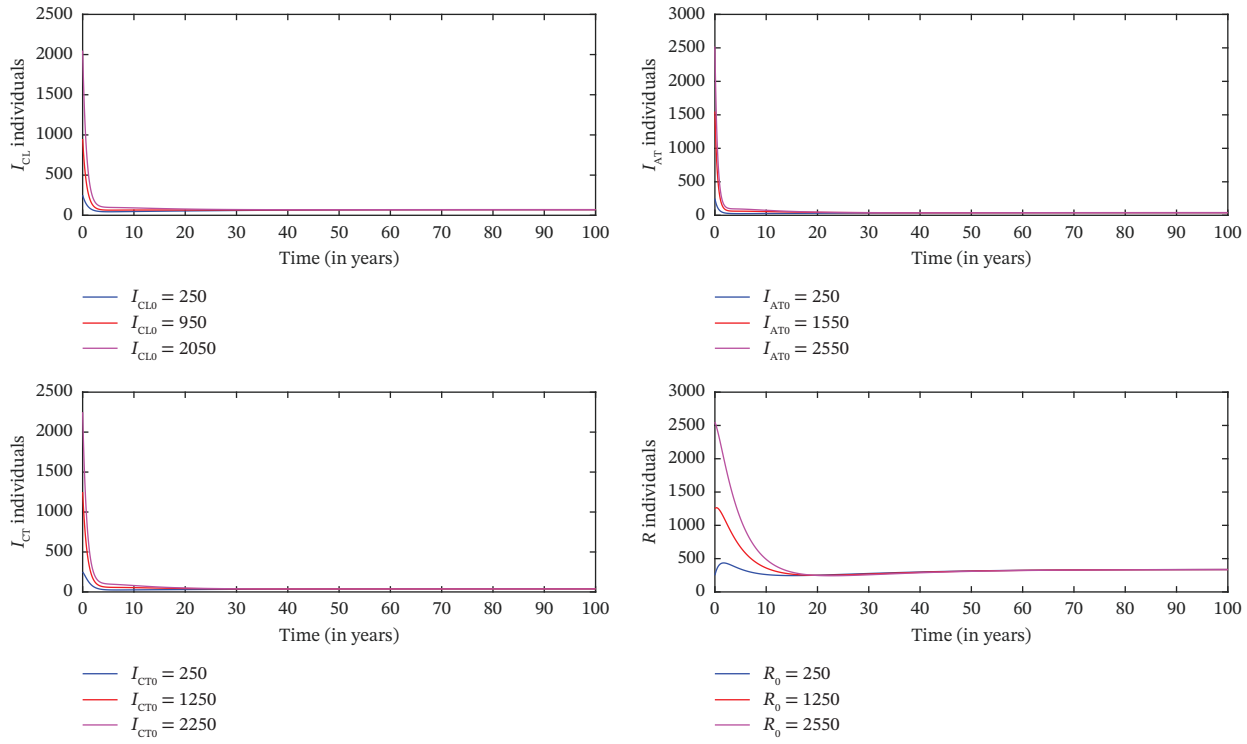


FIGURE 2 | The number of coinfected individuals against time.

increases (or decreases) with the rest of other parameter values maintained constant, the related effective reproduction number increases (or decreases). On the other hand, when a parameter with a negative sensitivity index increases (or decreases) with other parameter values kept constant, the associated effective reproduction number decreases (or increases).

For instance, raising (or lowering) the value of the rate of human-to-human contact between the TB infected individuals and susceptible population, ξ_1, by 20% while other parameters are kept constant, raises (lowers) the value of R_{TB} by 20%. Then, increasing (or decreasing) the value of the rate of natural recovery η, of TB latent individuals by 10% while keeping the values

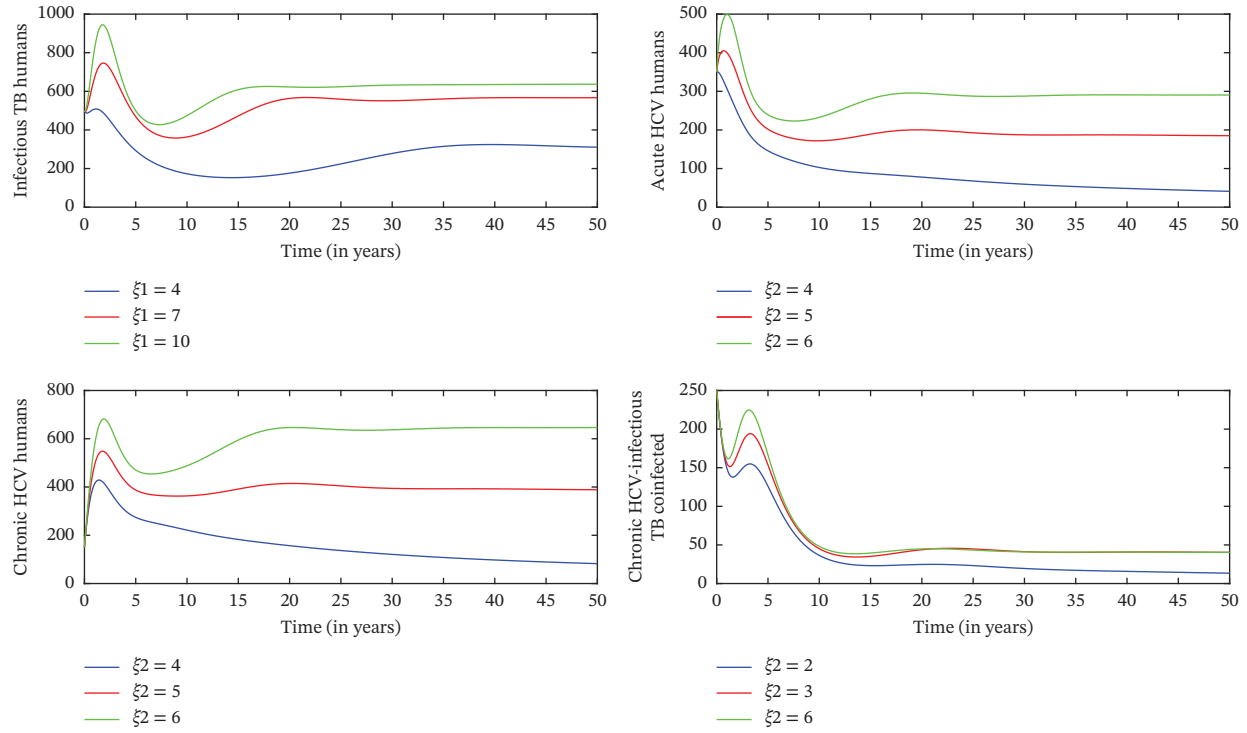


FIGURE 3 | The number of infectious TB, acute HCV, chronic HCV and chronic HCV-infectious TB coinfected individuals against time with ξ_1 and ξ_2, respectively, varied.

4185, 2026, 1, Downloaded from https://onlinelibrary.wiley.com/doi/10.1155/jama/8033235 by Readcube (Labtiva Inc.), Wiley Online Library on [12/11/2026]. See the Terms and Conditions (https://onlinelibrary.wiley.com/terms-and-conditions) on Wiley Online Library for rules of use; OA articles are governed by the applicable Creative Commons License

TABLE 3 | Numerical values for the sensitivity indices of R_{TB} and R_{HCV} with respect to parameters.

Effective reproduction number	Parameter	Sensitivity index
R_{TB}	ξ_1	1.0000
	q_1	1.0000
	ω_1	−0.8600
	θ	0.6481
	η	−0.6200
	ω_2	−0.5610
	σ_1	−0.0676
	σ_2	−0.0366
	ρ	−0.0312
	ϵ	0.0160
R_{HCV}	ξ_2	1.0000
	q_2	1.0000
	δ	−0.6457
	ψ	−0.2362
	π	−0.1179
	ϕ	0.1023
	α	0.0243

of other parameters constant, decreases (or increases) the value of R_{TB} by 6.2%. Comparably, the sensitivity indices of all other parameters can be explained.

Therefore, we conclude that the prevalence of TB infection increases when the values of the rate of human-to-human contact between the TB infected individuals and susceptible population ξ_1, the likelihood of a contact resulting in TB transmission q_1 and the rate of progression of individuals from latent to active stage θ are increased. However, the prevalence is observed to decrease when the values of the rate of treatment of TB infectious individuals ω_1, the rate of natural recovery of TB latent individuals η, the rate of hospitalisation of TB infectious individuals ρ, per capita natural mortality rate μ and the rate at which the hospitalised TB infectious individuals are put on treatment ω_2 are increased. The key factors of TB infection are ξ_1 and q_1 which are just as sensitive, followed by θ.

From Table 3, it is deduced that HCV infection becomes more prevalent when the values of rate of human-to-human contact between the HCV infected individuals and susceptible population ξ_2, the likelihood of a contact resulting in HCV transmission q_2, transmission coefficient for the acute HCV individuals ϕ and the rate of progression of individuals from acute to chronic HCV stage α are increased while those of rate at which chronic HCV individuals are put on treatment ψ, rate at which the chronic HCV die δ, natural recovery rate for the acute HCV humans π and the per capita natural mortality rate μ are decreased. The key factors of HCV infection are ξ_2 and q_2 which have equal sensitivity, followed by ϕ and α.

Therefore, efforts should focus on decreasing the values of ξ_2, q_2, ϕ and α.

Therefore, for reduced transmission of TB (or HCV) infection, interventions like health education campaigns involving screening and isolation of the infectious individuals, wearing masks by TB infectious individuals (or screening, sterilisation of surgical instruments and condom use for HCV infectious individuals) should be implemented. Also, seeking for early treatment of TB (or HCV) infectious individuals should be encouraged for those that test positive of TB (or HCV) infection.

Computation of R_{TH}: Inserting the parameter values from Table 2 into Equations (34) and (98), the values of $R_{TB} = 1.9407$ and $R_{HCV} = 1.1521$ are yielded.

From Equation (139), the effective reproduction number of the TB–HCV coinfection model is determined as follows:

$$R_{TH} = \max\{R_{TB}, R_{HCV}\} = \max\{1.9407, 1.1521\} = 1.9404. \quad (152)$$

Since $R_{TB} > R_{HCV}$, this implies that the interaction between TB and HCV infections in coinfected individuals is dominated by TB infection. This indicates that TB infection is more prevalent than HCV infection in a given community. This would mean more attention given to TB infection if the coinfection burden is to be reduced.

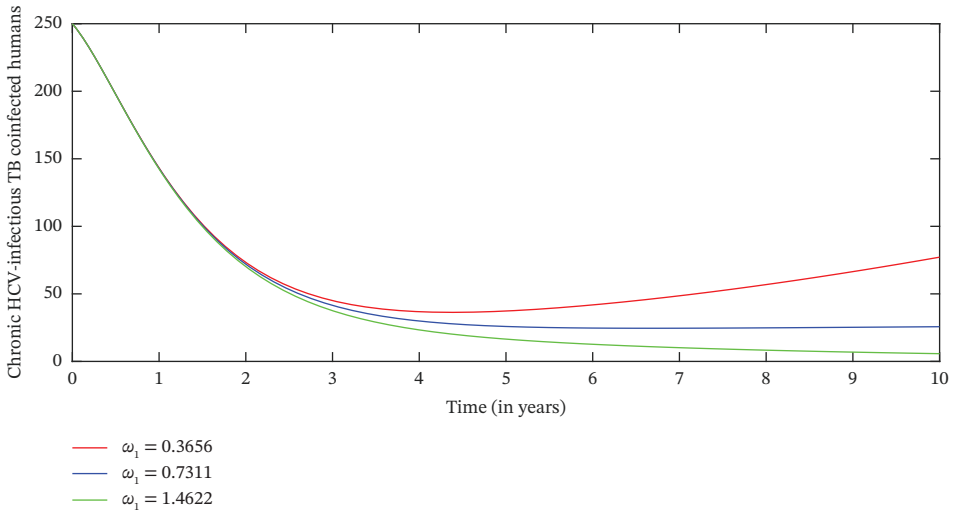


FIGURE 4 | The number of chronic HCV-infectious TB coinfected humans against time with TB treatment rate, ω_1, varied.

4185, 2026, 1, Downloaded from https://onlinelibrary.wiley.com/doi/10.1155/jama/8033235 by Readcube (Labtiva Inc.), Wiley Online Library on [12/11/2026]. See the Terms and Conditions (https://onlinelibrary.wiley.com/terms-and-conditions) on Wiley Online Library for rules of use; OA articles are governed by the applicable Creative Commons License

4.3 | Numerical Discussion

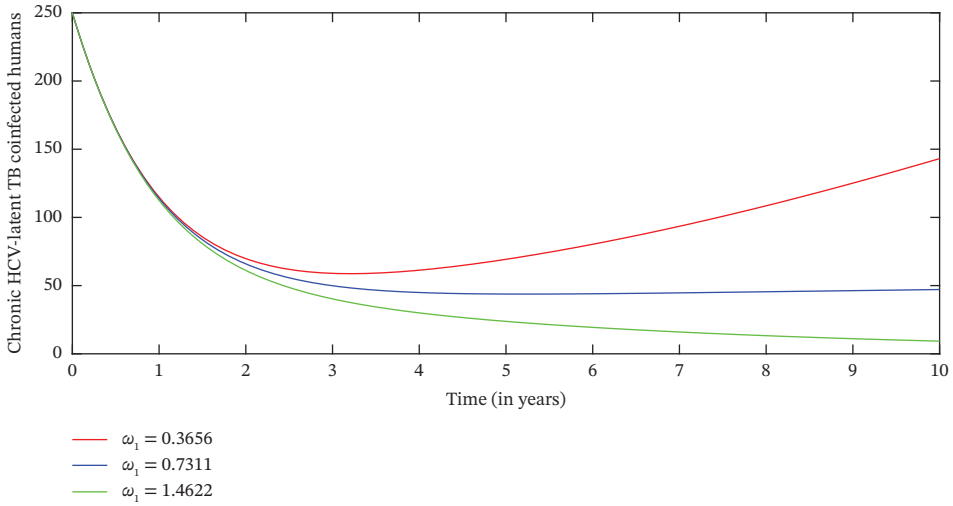
In the preceding sections, we have examined the analytical dynamics and characteristics of TB–HCV coinfection model with treatment as well as the submodels. Here, we carry out numerical simulations to validate and support the analytical findings, providing a deeper understanding of the TB–HCV coinfection dynamics with treatment. Assuming the initial values of the state variables as $S(0) = 40,000, I_L(0) = 500, I_T(0) = 450, H(0) = 250, R_T(0) = 500, I_A(0) = 350, I_C(0) = 400, R_H(0) = 350, I_{AL}(0) = 250, I_{CL}(0) = 250, I_{AT}(0) = 250, I_{CT}(0) = 250$ and $R(0) = 250$. A number of parameters have been obtained from existing literature, that is, $\mu, \sigma_1, \sigma_2, \delta, \theta, \rho, \omega_1, \omega_2, \alpha, \psi, \nu_1, \nu_3, \eta$ and π, as described in Table 2. Other parameters were carefully assumed depending on the dynamics of the coinfection, for example, $\tau_2 > \tau_1$ implying that I_{CL} individuals are more likely to progress to I_{CT} than I_{AL} progressing to I_{AT}. Similarly, the progression rate, β_2 from I_{AT} to I_{CT}, is greater than the progression rate, β_1 from I_{AL} to I_{CL}, since I_{AT} is more infectious of TB than I_{AL}. MATLAB software was employed to simulate the model using the ODE 45 solver. Both cases for $R_{TH} < 1$ and $R_{TH} > 1$ are catered for with parameter modification.

4.4 | Effect of Treating TB on the Coinfection Dynamics of TB and HCV

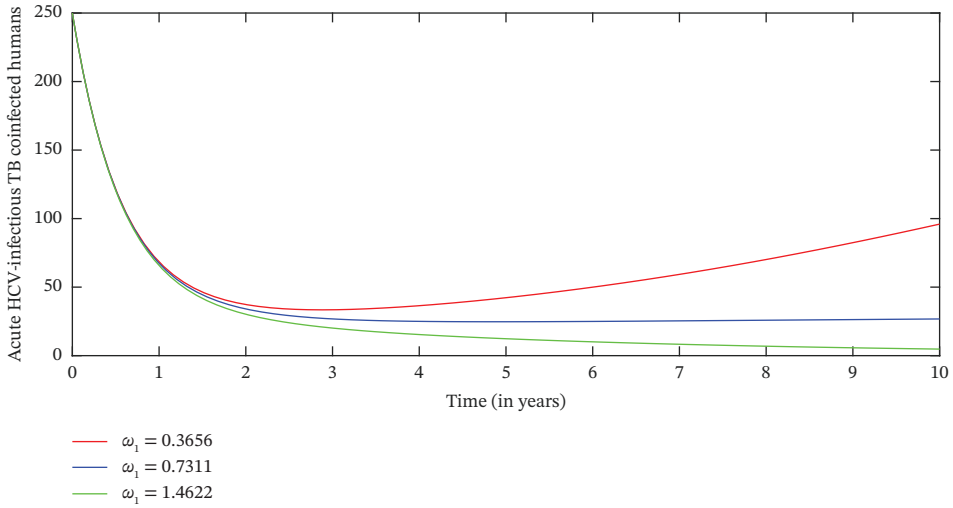
The results presented in Figure 4 indicate that enhancing the TB treatment rate leads to a substantial decrease in the prevalence of chronic HCV-infectious TB coinfected humans. Furthermore, in Figures 5(a) and 5(b), a similar decreasing trend is observed in the populations of humans coinfected with chronic HCV-latent TB, as well as people with acute HCV and infectious TB coinfection.

4.5 | Effect of Hospitalisation on the Coinfection Dynamics of TB and HCV

Figure 6 illustrates that enhancing the TB hospitalisation rate yields a proportional and substantial reduction in the number of humans with chronic HCV-infectious TB coinfection. Consistent



(a)



(b)

FIGURE 5 | The number of chronic HCV-latent TB coinfected humans against time, and number of acute HCV-infectious TB coinfected humans against time with TB treatment rate ω_1 varied. (a) The number of chronic HCV-latent TB coinfected humans against time with TB treatment rate ω_1 varied. (b) The number of acute HCV-infectious TB coinfected humans against time with TB treatment rate ω_1 varied.

4185, 2026, 1, Downloaded from https://onlinelibrary.wiley.com/doi/10.1155/jama/8033235 by Readcube (Labtiva Inc.), Wiley Online Library on [12/11/2026]. See the Terms and Conditions (https://onlinelibrary.wiley.com/terms-and-conditions) on Wiley Online Library for rules of use; OA articles are governed by the applicable Creative Commons License

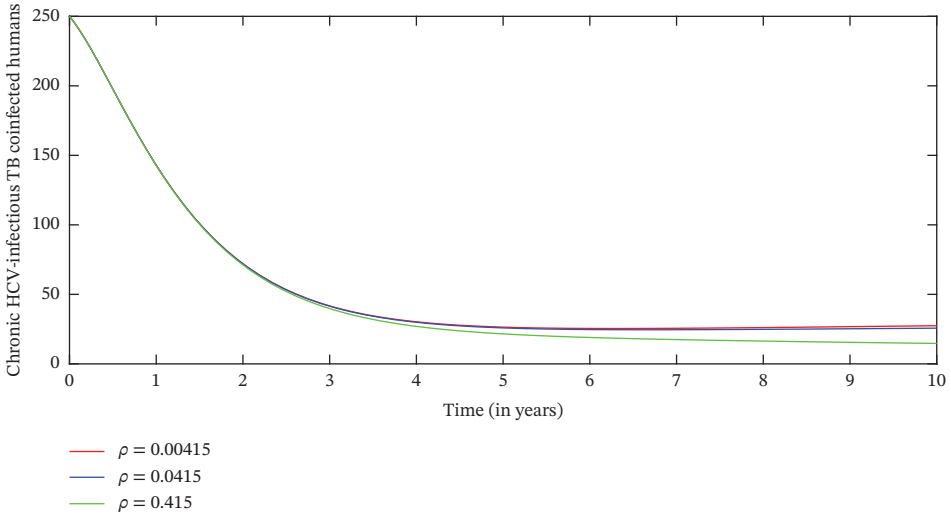
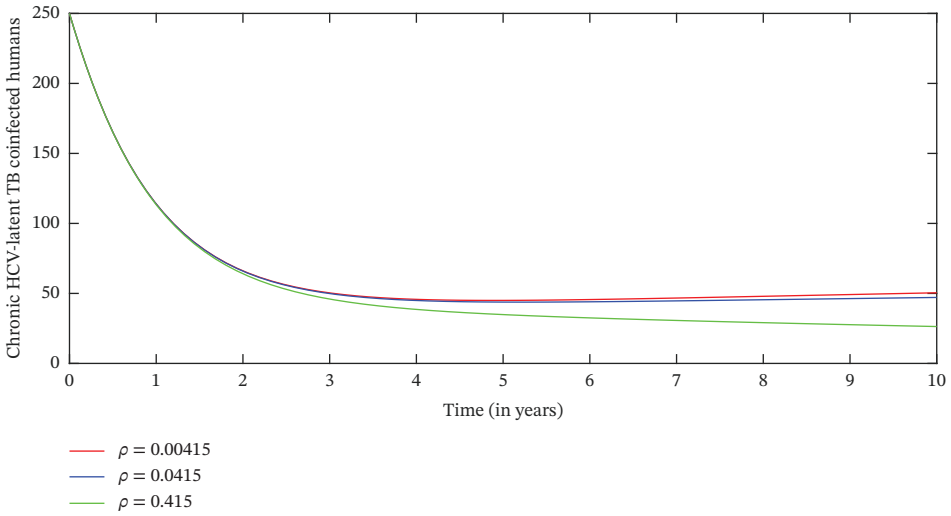
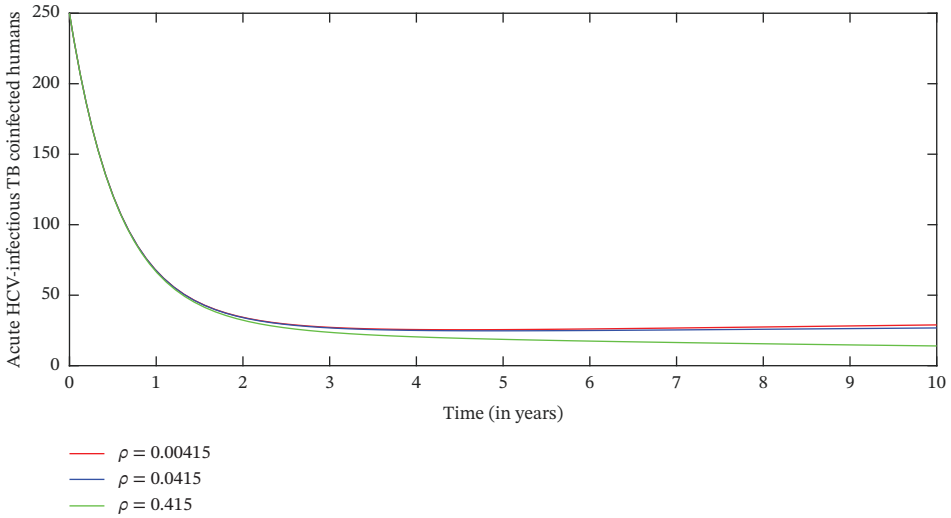


FIGURE 6 | The number of chronic HCV-infectious TB coinfected humans against time with hospitalisation rate, ρ varied.



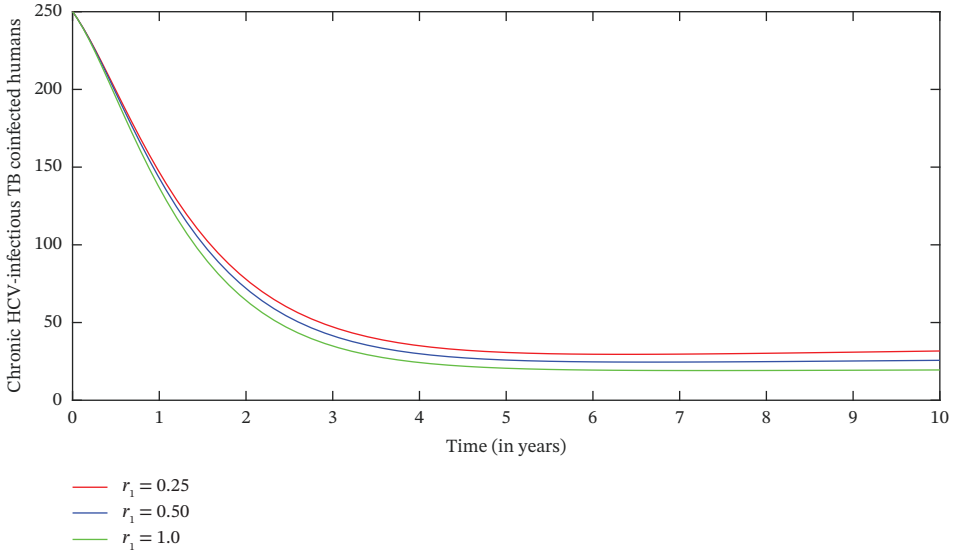
(a)



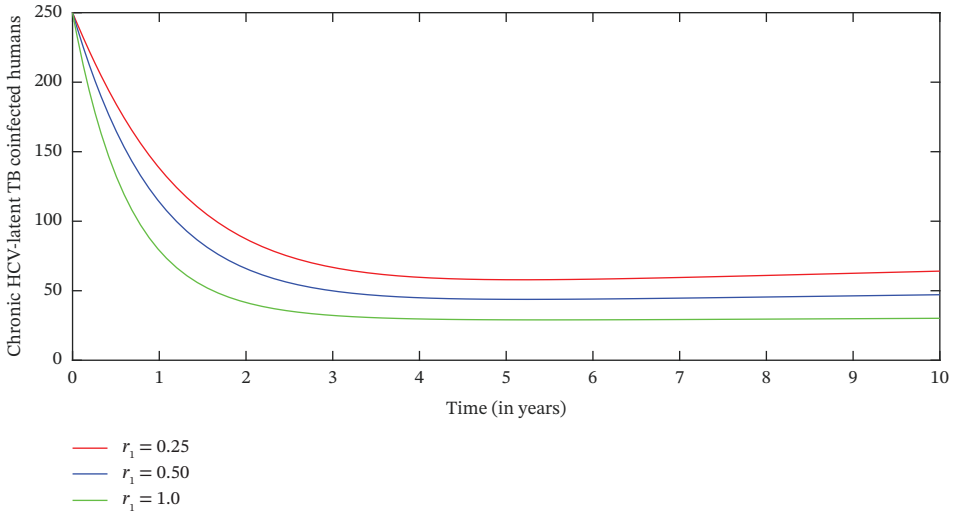
(b)

FIGURE 7 | The number of chronic HCV-latent TB coinfected humans against time, and number of acute HCV-infectious TB coinfected humans against time with hospitalisation rate ρ varied. (a) The number of chronic HCV-latent TB coinfected humans against time with hospitalisation rate ρ varied. (b) The number of acute HCV-infectious TB coinfected humans against time with hospitalisation rate ρ varied.

4185, 2026, 1, Downloaded from https://onlinelibrary.wiley.com/doi/10.1155/jama/8033235 by Readcube (Labtiva Inc.), Wiley Online Library on [12/11/2026]. See the Terms and Conditions (https://onlinelibrary.wiley.com/terms-and-conditions) on Wiley Online Library for rules of use; OA articles are governed by the applicable Creative Commons License

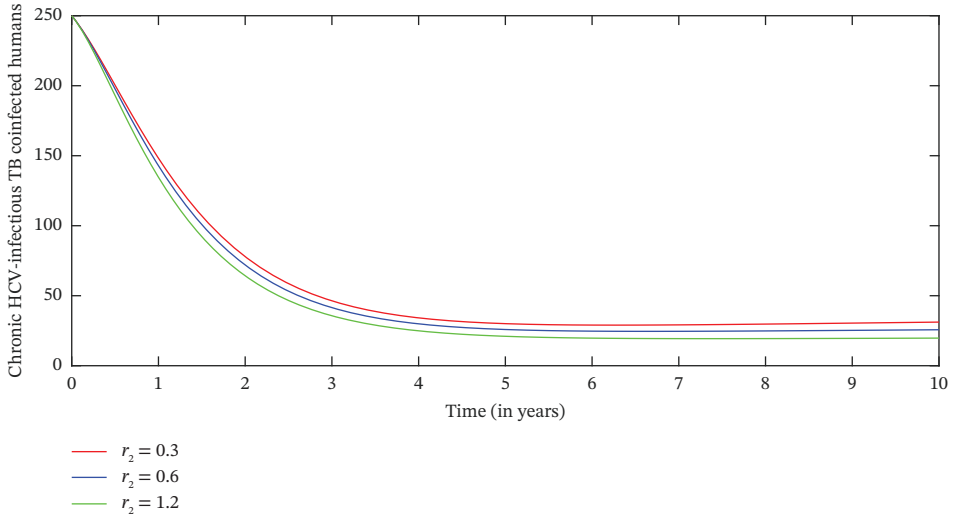


(a)



(b)

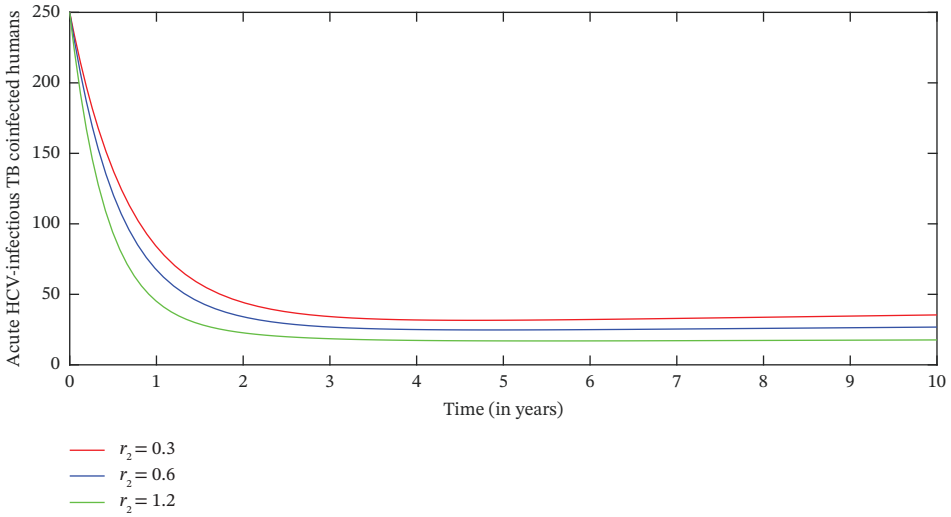
FIGURE 8 | The number of chronic HCV-latent TB coinfected humans against time, and number of acute HCV-infectious TB coinfected humans against time with HCV treatment rate, r_1 varied. (a) The number of chronic HCV-infectious TB coinfected humans against time with HCV treatment rate, r_1 varied. (b) The number of acute HCV-infectious TB coinfected humans against time with HCV treatment rate, r_1 varied.



(a)

FIGURE 9 | (Continued)

4185, 2026, 1, Downloaded from https://onlinelibrary.wiley.com/doi/10.1155/jama/8033235 by Readcube (Labtiva Inc.), Wiley Online Library on [12/11/2026]. See the Terms and Conditions (https://onlinelibrary.wiley.com/terms-and-conditions) on Wiley Online Library for rules of use; OA articles are governed by the applicable Creative Commons License



(b)

FIGURE 9 | The number of chronic HCV- latent TB coinfected humans against time, and number of acute HCV-infectious TB coinfected humans against time with TB treatment rate, r_2 varied. (a) The number of chronic HCV-infectious TB coinfected humans against time with TB treatment rate, r_2 varied. (b) The number of acute HCV-infectious TB coinfected humans against time with TB treatment rate, r_2 varied.

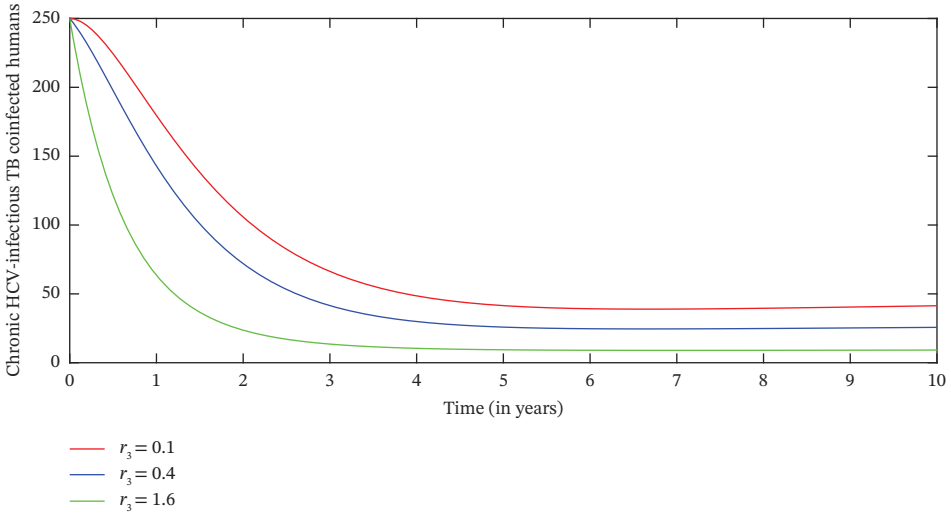


FIGURE 10 | The number of chronic HCV-infectious TB coinfected humans against time with treatment rate, r_3 varied.

with the trend observed in Figure 6, Figures 7a and 7b demonstrate that the populations of humans coinfected with chronic HCV and latent TB, and those coinfected with acute HCV and infectious TB, also show a corresponding decline.

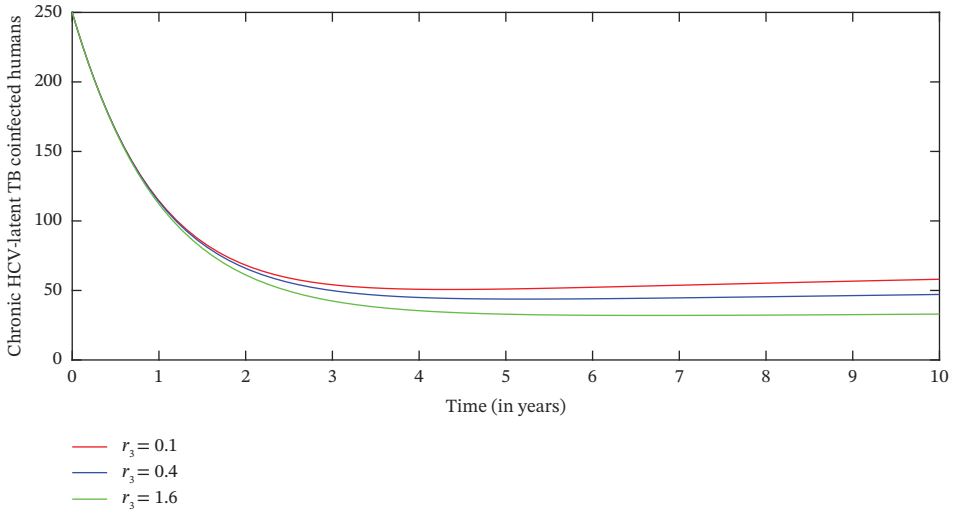
4.6 | Role of Treatment Rates, r_1, r_2 and r_3 on the Coinfection Dynamics of TB and HCV

Figures 8(a), 8(b), 9(a), 9(b) indicate that when the rates r_1 and r_2, respectively, at which humans are put on HCV and TB medication rise, the number of people infected by chronic HCV-infectious TB and chronic HCV-latent TB coinfection decreases. Similarly, Figures 10, 11(a), and 11(b) reveal that increasing the rate r_3, respectively, at which humans are put on TB and HCV medical treatment, decreases the number of chronic HCV-latent TB coinfected humans and acute HCV-infectious TB coinfected humans.

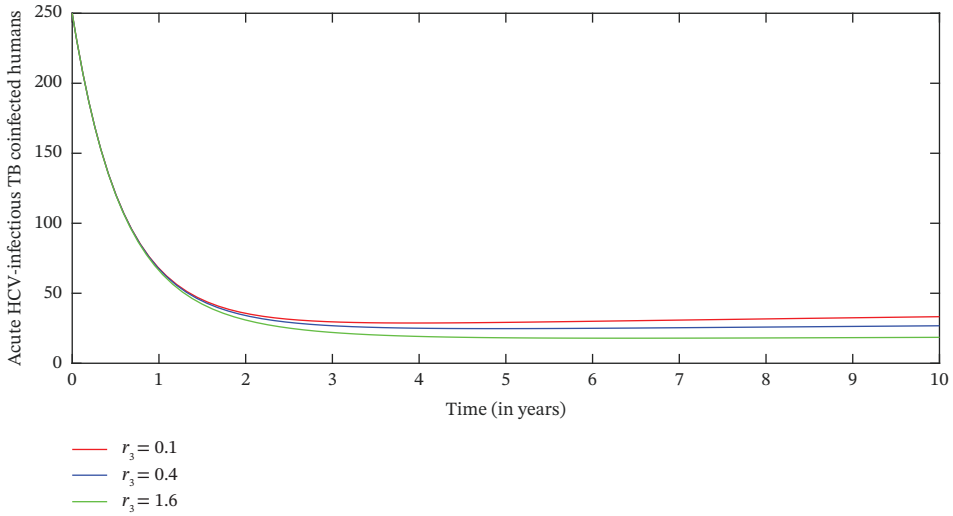
4.7 | Effect of Treating HCV on the Coinfection Dynamics of TB and HCV

Figure 12 demonstrates that enhancing the HCV treatment rate yields a proportional and substantial reduction in the number of humans with chronic HCV-infectious TB coinfection. Consistent

4185, 2026, 1, Downloaded from https://onlinelibrary.wiley.com/doi/10.1155/jama/8033235 by Readcube (Labtiva Inc.), Wiley Online Library on [12/11/2026]. See the Terms and Conditions (https://onlinelibrary.wiley.com/terms-and-conditions) on Wiley Online Library for rules of use; OA articles are governed by the applicable Creative Commons License



(a)



(b)

FIGURE 11 | The number of chronic HCV-latent TB coinfected humans against time, and number of acute HCV-infectious TB coinfected humans against time with treatment rate r_3 varied. (a) The number of chronic HCV-latent TB coinfected humans against time with treatment rate r_3 varied. (b) The number of acute HCV-infectious TB coinfected humans against time with treatment rate r_3 varied.

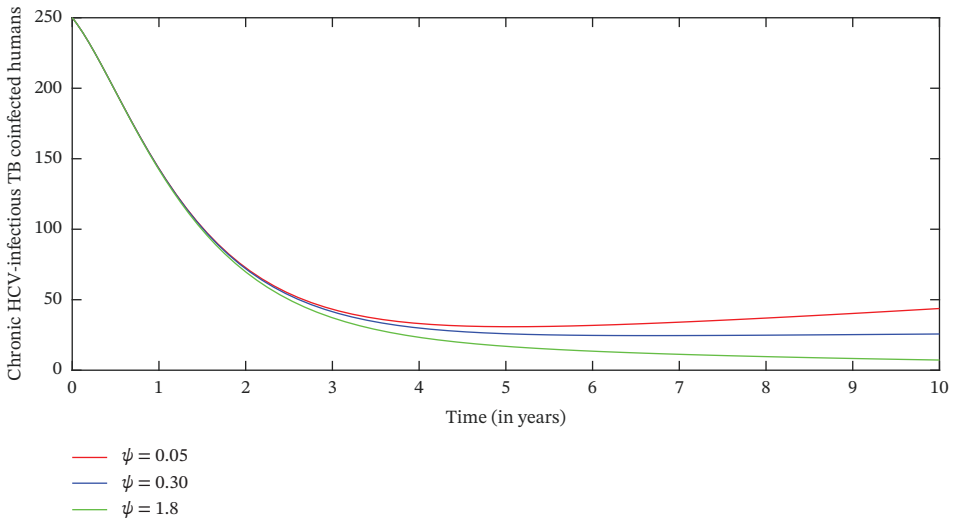
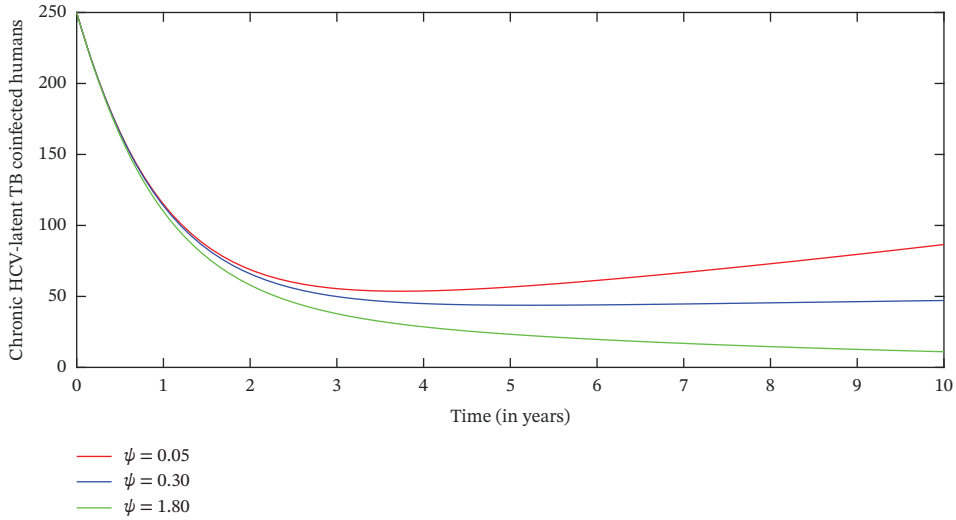
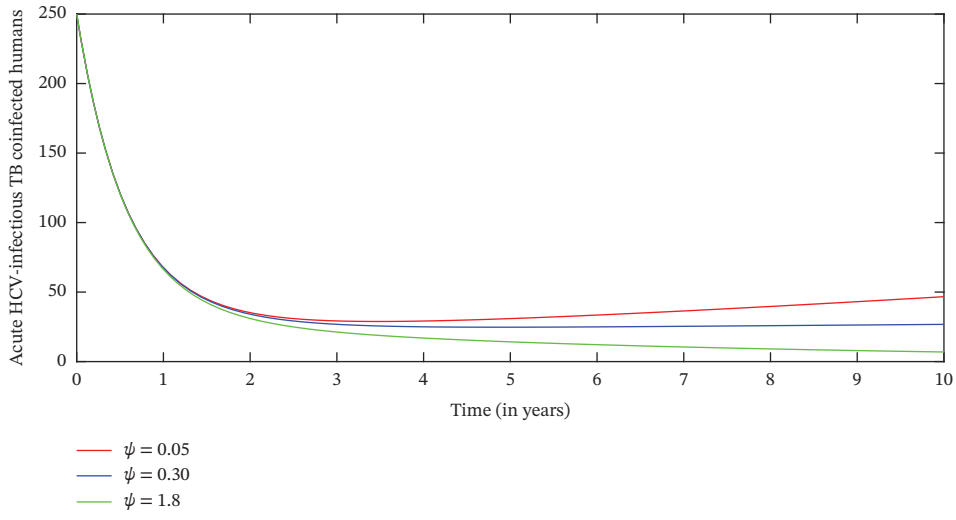


FIGURE 12 | The number of chronic HCV-infectious TB coinfected humans against time with HCV treatment rate, ψ, varied.

4185, 2026, 1, Downloaded from https://onlinelibrary.wiley.com/doi/10.1155/jama/8033235 by Readcube (Labtiva Inc.), Wiley Online Library on [12/11/2026]. See the Terms and Conditions (https://onlinelibrary.wiley.com/terms-and-conditions) on Wiley Online Library for rules of use; OA articles are governed by the applicable Creative Commons License



(a)



(b)

FIGURE 13 | The number of chronic HCV-latent TB coinfected humans against time, and number of acute HCV-infectious TB coinfected humans against time with HCV treatment rate ψ varied. (a) The number of chronic HCV-latent TB coinfected humans against time with HCV treatment rate ψ varied. (b) The number of acute HCV-infectious TB coinfected humans against time with HCV treatment rate ψ varied.

with the trend observed in Figure 12, Figures 13a and 13b demonstrate a decline in the populations of individuals coinfected with chronic HCV and latent TB and those coinfected with acute HCV and infectious TB.

5 | Conclusion

This study developed and analysed a mathematical model to investigate the behaviour of TB and HCV coinfection with medication, extending the previous work in reference [39]. The model was intended to assess the impact of the medication on the progression of TB and HCV coinfection. Under medication for both TB and HCV, the intricate dynamics of TB–HCV coinfection is dominated by TB. From sensitivity analysis, it is deduced that the rate of human-to-human contact between the TB (or HCV) infectious individuals and susceptible population and the likelihood of a contact resulting in TB (or HCV) transmission have an equal potential to lead to an increase in TB (or HCV) cases. Furthermore, enhancing these parameters also boosts TB (or HCV) infection levels. Our results are consistent with the findings of reference [39], which explored the dynamics of TB–HCV coinfection without intervention for either infection. Therefore, we recommend that for decreased TB (or HCV) infections, there is a need to greatly reduce the rate of human-to-human contact between the TB (or HCV) infectious individuals and susceptible population. Numerical simulation results unequivocally reveal that over time, increasing the TB treatment rate, HCV treatment rate, hospitalisation rate and the rates at which individuals in coinfected classes are identified and put on TB and HCV treatment can significantly reduce the prevalence of TB–HCV coinfection. Implementing the above interventions can have a profound impact on reducing the burden of the coinfection and thus improving public health outcomes. We, therefore, recommend that health facilities be stocked with antibiotics for TB and antiviral medications for easy access to individuals who taste positive to the respective infections. This study can be further expanded to include optimal control strategies and evaluate the cost-effectiveness of the different

4185, 2026, 1, Downloaded from https://onlinelibrary.wiley.com/doi/10.1155/jama/8033235 by Readcube (Labtiva Inc.), Wiley Online Library on [12/11/2026]. See the Terms and Conditions (https://onlinelibrary.wiley.com/terms-and-conditions) on Wiley Online Library for rules of use; OA articles are governed by the applicable Creative Commons License

control strategies. The model in this study can also be improved by incorporating time delays in the treatment process such as delays in diagnosis, treatment initiation and treatment completion.

Funding

No funding was obtained for this study.

Conflicts of Interest

The authors declare no conflicts of interest.

Data Availability Statement

The data used are obtained from existing literature that is cited.

References

1. World Health Organization, "Global Tuberculosis Report 2019," in *Global Tuberculosis Report 2019* (2019).

2. J. W. Ai, Q. L. Ruan, Q. H. Liu, and W. H. Zhang, "Updates on the Risk Factors for Latent Tuberculosis Reactivation and Their Managements," *Emerging Microbes & Infections* 5, no. 1 (2016): 1–8.

3. A. Fares, "Seasonality of Tuberculosis," *Journal of Global Infectious Diseases* 3, no. 1 (2011): 46–55.

4. World Health Organization, *WHO Consolidated Guidelines on Tuberculosis: Module 4: Treatment: Drug-Susceptible Tuberculosis Treatment: Web Annexes* (World Health Organization, 2022).

5. H. Wan, R. L. Adams, B. D. Lindenbach, and A. M. Pyle, "The in Vivo and in Vitro Architecture of the Hepatitis C Virus RNA Genome Uncovers Functional RNA Secondary and Tertiary Structures," *Journal of Virology* 96, no. 8 (2022): e01946.

6. E. Robinson, C. J. Byrne, J. Carberry, et al., "Laying the Foundations for Hepatitis C Elimination: Evaluating the Development and Contribution of Community Care Pathways to Diagnostic Efforts," *BMC Public Health* 23, no. 1 (2023): 54.

7. S. E. Schröeder, A. Pedrana, N. Scott, et al., "Innovative Strategies for the Elimination of Viral Hepatitis at a National Level: A Country Case Series," *Liver International* 39, no. 10 (2019): 1818–1836.

8. J. Grebely, G. J. Dore, S. Morin, J. K. Rockstroh, and M. B. Klein, "Elimination of HCV as a Public Health Concern Among People Who Inject Drugs by 2030–What Will It Take to Get There?" *Journal of the International AIDS Society* 20, no. 1 (2017): 22146.

9. S. Schillie, C. Wester, M. Osborne, L. Wesolowski, and A. B. Ryerson, "CDC Recommendations for Hepatitis C Screening Among Adults—United States, 2020," *Morbidity and Mortality Weekly Report Recommendations and Reports* 69, no. 2 (2020): 1.

10. World Health Organization, *Guidelines for the Screening Care and Treatment of Persons With Chronic Hepatitis C Infection Updated Version April 2016: Guidelines* (World Health Organization, 2016).

11. M. Hickman, N. K. Martin, I. Giraudon, et al., *Hepatitis C Among Drug Users in Europe: Epidemiology, Treatment and Prevention* (Publication Office of the European Union, 2016).

12. S. Zhang and Y. Zhou, "Dynamics and Application of an Epidemiological Model for Hepatitis C," *Mathematical and Computer Modelling* 56, no. 1-2 (2012): 36–42.

13. F. Cui, S. Blach, C. M. Mingiedi, et al., "Global Reporting of Progress Towards Elimination of Hepatitis B and Hepatitis C," *Lancet Gastroenterology & Hepatology* 8, no. 4 (2023): 332–342.

14. S. E. Karimi, A. Bayani, P. Higgs, et al., "Prevalence and High Risk Behaviours Associated With HCV Testing Among People Who Inject Drugs: A Systematic Review and Meta-Analysis," *Substance Abuse Treatment, Prevention, and Policy* 15, no. 1 (2020): 1–16.

15. M. Baluku, T. Wamala, and D. Muhangi, "HIV-and Hepatitis C-Related Risk Behaviors Among People Who Inject Drugs in Uganda: Implications for Policy and Programming," *Harm Reduction Journal* 16 (2019): 1–7.

16. E. Mayanja, L. S. Luboobi, J. Kasozi, and R. N. Nsubuga, "Mathematical Modelling of HIV-HCV Co-infection Dynamics in Presence of HIV Therapy," *Bio-Mathematics* 11, no. 1 (2022): 2207158.

17. J. I. O'reilly, P. Ocama, C. K. Opio, et al., "Risk factors and seroprevalence of hepatitis C among patients hospitalized at Mulago Hospital, Uganda," *Journal of Tropical Medicine* 2011 (2011).

18. B. Meysam, S. Heydarvand, M. Behzadifar, and N. L. Bragazzi, "Prevalence of Hepatitis C Virus in Tuberculosis Patients: A Systematic Review and Meta-Analysis," *Ethiopian Journal of Health Sciences* 29, no. 1 (2019).

19. M. Ronoh, R. Jaroudi, P. Fotso, et al., "A Mathematical Model of Tuberculosis With Drug Resistance Effects," *Applied Mathematics* 7, no. 12 (2016): 1303–1316.

20. J. Zhang, Y. Li, and X. Zhang, "Mathematical Modeling of Tuberculosis Data of China," *Journal of Theoretical Biology* 365 (2015): 159–163.

21. M. A. K. Fatmawati, E. Bonyah, Z. Hammouch, and E. M. Shaiful, "A Mathematical Model of Tuberculosis (TB) Transmission With Children and Adults Groups: A Fractional Model," *Aims Math* 5, no. 4 (2020): 2813–2842.

22. M. Altaf Khan, K. Khan, M. A. Safi, and M. H. DarAssi, "A Discrete Model of TB Dynamics in Khyber Pakhtunkhwa-Pakistan," *Computer Modeling in Engineering and Sciences* 123, no. 2 (2020): 777–795.

23. R. Shi and Y. Cui, "Global Analysis of a Mathematical Model for Hepatitis C Virus Transmissions," *Virus Research* 217 (2016): 8–17.

24. T. Megala, T. Nandha Gopal, M. Siva Pradeep, M. Sivabalan, and A. Yasotha, "Dynamics of Re-Infection in a Hepatitis B Virus Epidemic Model With Constant Vaccination and Preventive Measures," *Journal of Applied Mathematics and Computing* (2025): 1–27.

25. C. Nino, N. Rukhadze, M. Svanidze, et al., "Evaluation of Multiple Measures of Antiretroviral Adherence in the Eastern European Country of Georgia," *African Journal of Reproduction and Gynaecological Endoscopy* 17, no. 1 (2014).

26. M. A. El-Mokhtar, S. G. Elgendy, A. S. Eldin, et al., "Hepatitis C Virus Affects Tuberculosis-Specific T Cells in HIV-Negative Patients," *Viruses* 12, no. 1 (2020): 101.

27. M. Musso, S. Mosti, G. Gualano, et al., "Hepatitis C Virus Infection: A Challenge in the Complex Management of Two Cases of Multidrug-Resistant Tuberculosis," *BMC Infectious Diseases* 19 (2019): 1–4.

28. E. S. Nageeb, S. M. Abu-Bakr, H. A. Eid, and H. A. Abou Elhassan, "Impact of Hepatitis C Virus Co-Infection on Tuberculous Patients," *International Journal of Medical Arts* 3, no. 4 (2021): 1884–1890.

29. B. Wahid, K. Saleem, M. Waqar, M. Wasim, and M. Idrees, "Successful Treatment of HCV/TB Co-Infected Patient With Sofosbuvir and Daclatasvir: A Case Report," *Future Virology* 13, no. 5 (2018): 317–321.

30. R. R. Kempker, W. A. Alghamdi, M. H. Al-Shaer, G. Burch, and C. A. Peloquin, "A Pharmacology Perspective on Simultaneous Tuberculosis and Hepatitis C Treatment," *Antimicrobial Agents and Chemotherapy* 63, no. 12 (2019): 10–1128.

31. R. Aggarwal, "Stability Analysis of a Delayed HIV-TB Co-Infection Model in Resource Limitation Settings," *Chaos, Solitons & Fractals* 140 (2020): 110138.

32. S. Bowong and J. Kurths, "Modelling Tuberculosis and Hepatitis B co-infections," *Mathematical Modelling of Natural Phenomena* 5, no. 6 (2010): 196–242.

33. A., R. Tanvi and T. Kovacs, "Assessing the Effects of Holling Type-II Treatment Rate on HIV-TB Co-Infection," *Acta Biotheoretica* 69 (2021): 1–35.

4185, 2026, 1, Downloaded from https://onlinelibrary.wiley.com/doi/10.1155/jama/8033235 by Readcube (Labtiva Inc.), Wiley Online Library on [12/11/2026]. See the Terms and Conditions (https://onlinelibrary.wiley.com/terms-and-conditions) on Wiley Online Library for rules of use; OA articles are governed by the applicable Creative Commons License

34. C. P. Bhunu and S. Mushayabasa, "Modelling the Transmission Dynamics of HIV/AIDS and Hepatitis C Virus Co-Infection," *HIV & AIDS Review* 12, no. 2 (2013): 37–42.

35. S. W. Teklu, Y. F. Abebaw, B. B. Terefe, and D. K. Mamo, "HIV/AIDS and TB Co-Infection Deterministic Model Bifurcation and Optimal Control Analysis," *Informatics in Medicine Unlocked* 41 (2023): 101328.

36. H. Nampala, M. Jablonska-Sabuka, and M. Singull, "Mathematical Analysis of the Role of HIV/HBV Latency in Hepatocytes," *Journal of Applied Mathematics* 2021 (2021): 1–15.

37. S. W. Teklu and Y. F. Abebaw, "Analysis of the HBV and TB Coinfection Model With Optimal Control Strategies and Cost-Effectiveness," *Discrete Dynamics in Nature and Society* 2024, no. 1 (2024): 8811930.

38. R. Aggarwal, "Estimating the Impact of Antiretroviral Therapy on HIV-TB Co-Infection: Optimal Strategy Prediction," *International Journal of Biomathematics* 14, no. 01 (2021): 2150004.

39. M. Kizito, H. Nampala, and P. Ariho, "Mathematical Modelling of Tuberculosis and Hepatitis C Coinfection Dynamics With No Intervention," *Journal of Mathematics* 2024 (2024): 1–28.

40. S. Zhang and X. Xu, "Dynamic Analysis and Optimal Control for a Model of Hepatitis C With Treatment," *Communications in Nonlinear Science and Numerical Simulation* 46 (2017): 14–25.

41. A. Cintrón-Arias, C. Castillo-Chávez, L. M. Bettencourt, A. L. Lloyd, and H. T. Banks, "The Estimation of the Effective Reproductive Number from Disease Outbreak Data," *Mathematical Biosciences and Engineering* 6, no. 2 (2009): 261–282.

42. P. Van den Driessche and J. Watmough, "Reproduction Numbers and Sub-Threshold Endemic Equilibria for Compartmental Models of Disease Transmission," *Mathematical Biosciences* 180, no. 1 (2002): 29–48.

43. K. K. Pal, R. K. Rai, P. K. Tiwari, and A. K. Misra, "Role of Awareness Programs on Diabetes Prevention and Control of Viral Infection: A Study of Optimal Control," *European Physical Journal Plus* 140, no. 2 (2025): 150.

44. C. Castillo-Chavez, Z. Feng, and W. Huang, "On the Computation of R_0 and Its Role on Global Stability" (2002).

45. M. Byamukama, D. Kajunguri, and M. Karuhanga, "Optimal Control Analysis of Pneumonia and HIV/AIDS Co-Infection Model," *Mathematics Open* 3 (2024): 2450006.

46. M. Kizito and J. Tumwiine, "A Mathematical Model of Treatment and Vaccination Interventions of Pneumococcal Pneumonia Infection Dynamics," *Journal of Applied Mathematics* 2018 (2018).

47. J. P. LaSalle, "The Stability of Dynamical Systems," *Regional Conference Series in Applied Mathematics, Society for Industrial and Applied Mathematics* (American Naturalist, 1976), 79–99.

48. M. Byamukama, M. Karuhanga, and D. Kajunguri, "Mathematical Analysis of the Role of Treatment and Vaccination in the Management of the HIV/AIDS and Pneumococcal Pneumonia Co-Infection," *Journal of Mathematics* 2025, no. 1 (2025): 5879698.

49. Z. Feng, C. Castillo-Chavez, and A. F. Capurro, "A Model for Tuberculosis With Exogenous Reinfection," *Theoretical Population Biology* 57, no. 3 (2000): 235–247.

50. J. Q. Zhao, E. Bonyah, B. Yan, et al., "A Mathematical Model for the Coinfection of Buruli Ulcer and Cholera," *Results in Physics* 29 (2021): 104746.

51. K. O. Okosun, M. A. Khan, E. Bonyah, and O. O. Okosun, "Cholera-Schistosomiasis Coinfection Dynamics," *Optimal Control Applications and Methods* 40, no. 4 (2019): 703–727.

52. N. Chitnis, J. M. Hyman, and J. M. Cushing, "Determining Important Parameters in the Spread of Malaria Through the Sensitivity Analysis of a Mathematical Model," *Bulletin of Mathematical Biology* 70, no. 5 (2008): 1272–1296.

53. S. M. Blower and H. Dowlatabadi, "Sensitivity and Uncertainty Analysis of Complex Models of Disease Transmission: An HIV Model, as an Example," *International Statistical Review/Revue Internationale de Statistique* (1994): 229–243.

54. N. Chitnis, J. M. Cushing, and J. M. Hyman, "Bifurcation Analysis of a Mathematical Model for Malaria Transmission," *SIAM Journal on Applied Mathematics* 67, no. 1 (2006): 24–45.

4185, 2026, 1, Downloaded from https://onlinelibrary.wiley.com/doi/10.1155/jama/8033235 by Readcube (Labtiva Inc.), Wiley Online Library on [12/11/2026]. See the Terms and Conditions (https://onlinelibrary.wiley.com/terms-and-conditions) on Wiley Online Library for rules of use; OA articles are governed by the applicable Creative Commons License